Sedimentologika
Research article

Geochronology of reworked ash and its implications for accommodation space variations in distal foreland basins, McMurray Formation, Alberta, Canada

Susanne W. Fietz[1,2*], Jim L. Crowley[3], James A. MacEachern[1], Shahin E. Dashtgard[1], H. Dan Gibson[4]

1 ARISE, Department of Earth Sciences, Simon Fraser University, Burnaby, British Columbia, V5A 1S6, Canada
2 Federal Institute for Geoscience and Natural Resources, B3.1 Subsurfaces Use, 30655 Hannover, Germany
3 Department of Geoscience, Boise State University, Boise, Idaho 83725, USA
4 P-T Group, Department of Earth Sciences, Simon Fraser University, Burnaby, British Columbia, V5A 1S6, Canada

*corresponding author: Susanne W. Fietz (susanne.fietz@bgr.de)
doi: 10.57035/journals/sdk.2023.e11.1131

Editors: Stéphane Bodin and Julien Bailleul
Reviewers: Dinu I. Pană, Martin Roddaz and Luca Caracciolo
Copyediting, layout and production: Romain Vaucher, Farid Saleh and Sophie Hage

Submitted: 20.03.2023
Accepted: 23.08.2023
Published: 05.10.2023

Abstract | A bentonite bed consisting of reworked volcanic ash from the Barremian to Aptian lower McMurray Formation is dated using chemical abrasion thermal ionization mass spectrometry (CA-TIMS) on zircon. The bentonite bed is from a cored interval in the McKay Paleovalley in the northern Athabasca Oil Sands Region of Alberta, Canada. Deposition of the lower McMurray Formation took place in the distal portion of the Western Canada Sedimentary Basin early in the Cretaceous-to-Paleocene phase of widespread contractional deformation in the Canadian Cordillera. A 30 g sample of volcanic ash yielded >10,000 very small (<50 µm) zircon grains with the vast majority (~99.7%) being highly abraded and clearly detrital. Twenty-six sharply faceted grains were sufficiently large to be mounted for laser ablation inductively coupled plasma mass spectrometry (LA-ICPMS) analysis, which yielded seven Lower Cretaceous dates. These Lower Cretaceous grains were further analyzed using CA-TIMS. The five youngest CA-TIMS dates agree with a weighted mean of 121.51 ± 0.11 Ma which is conservatively interpreted as a maximum depositional age (MDA). The good agreement between the five zircon dates indicates the MDA is probably the depositional age. This study demonstrates that with careful analysis of zircon populations, high-confidence MDAs can be derived even from reworked ash beds that are dominated overwhelmingly by detrital zircon. The date from this study overlaps a previously published MDA of 121.39 ± 0.27 Ma for the top of the lower McMurray Formation in Firebag Tributary in the northeastern Athabasca Oil Sands Area. The overlapping dates establish a widespread chronostratigraphic surface within the northern Athabasca Oil Sands Area. Both ages are from ash beds preserved in coal seams, suggesting that the coal-bearing interval is a regional marker bed and that the ash beds may form an intraformational datum. Further, the occurrence of the ash beds in the McMurray Formation in close proximity to regional flooding surfaces suggests that tectonic activity in the emerging Canadian Cordillera influenced accommodation space variations in the distal portions of the adjacent foreland basin.

Lay summary | Zircon from a highly reworked ash sample from the Aptian lower McMurray Formation was dated to establish a maximum depositional age (i.e., youngest age derived from dated minerals). The ash sample contained predominantly small and rounded detrital zircon. Five sharply faceted zircon returned a very narrow range of age dates, which can be interpreted as the ash bed's true depositional age. The results of this study permit the first chronostratigraphic correlation between sub-basins of the McMurray Formation and may indicate that tectonic processes contributed to accommodation space variations during its deposition.

Keywords: U-Pb, CA-TIMS, bentonite, Canadian Cordillera, Early Cretaceous

1. Introduction

Geochronology using zircon crystals from altered volcanic ash (bentonite) beds is a well-established method to determine high-confidence maximum depositional ages (e.g., Boltwood, 1907; Baadsgaard & Lerbekmo, 1983; Odin et al., 1991; Mattinson, 2005, 2010; Schoene, 2014; Condon et al., 2015; Schaltegger et al., 2015). The integration of geochronological data with sequence stratigraphy is a useful tool for underpinning local-, basin- and global-scale stratigraphic interpretations (e.g., Baadsgaard & Lerbekmo, 1983; Mitchell et al., 2004; Bhattacharya, 2011; Cohen et al., 2013; Huff, 2016; Lin et al., 2019; Rinke-Hardekopf et al., 2022). Ash beds can have significant sequence stratigraphic potential as marker beds because they are relatively easy to identify and correlate. As well, pyroclastic ash fall can be widespread and reflect geologically instantaneous events. In facies characterized by minimal topographic relief (e.g., coal and marine shale), such ash beds can serve as ideal datums (e.g., Wheeler & Mallory, 1953; Van Wagoner et al., 1990; Bhattacharya & Willis, 2001; Mitchell et al., 2004; Vakarelov & Bhattacharya, 2009).

In this study, single-zircon U-Pb age-dating techniques are applied to obtain a precise and accurate maximum depositional age (MDA) for a reworked ash bed from the lower McMurray Formation (Fm) in the McKay Paleovalley of the northern Athabasca Oil Sands Region (AOSR) of Alberta, Canada. The MDA is compared to previously published dates from the McMurray Fm. The geochronological data assist with stratigraphic correlations across geographically separated depocenters of the McMurray Fm, and have implications for the delineation of controlling factors on accommodation space creation in distal foreland basins.

The Barremian to Aptian McMurray Fm was deposited in the distal part of the Western Canada Sedimentary Basin (WCSB), which operated as a foreland basin east of the Canadian Cordillera since the Jurassic (Figure 1) (Porter et al., 1982; Price, 1994; Hein et al., 2012). The deposits comprise stacked and amalgamated fluvial to marginal marine successions that accumulated in an overall low-accommodation space setting during early onset of significant compression in the Early Cretaceous Canadian Cordillera (Carrigy, 1959; Pemberton et al., 1982; Keith et al., 1988; Ranger & Pemberton, 1992; Wightman & Pemberton, 1997; Baniak & Kingsmith, 2018; Monger & Gibson, 2019). Several lithostratigraphic and sequence stratigraphic models for the McMurray Fm have been proposed, but regional correlations remain ambiguous, owing to the complex depositional pattern and limited extent of intraformational marker horizons (Figure 2) (Carrigy, 1959; Ranger & Pemberton, 1997; Hein et al., 2012; Broughton, 2015; Horner et al., 2018; Château et al., 2021; Peng et al., 2022; Rinke-Hardekopf et al., 2022).

Distal foreland basins (i.e., distal foredeep to backbulge basins) are typically low-accommodation space settings in which sedimentation is widely regarded to be controlled primarily by eustatic sea level changes (see Cant & Stockmal, 1989; Ross et al., 2005; DeCelles, 2012; Horner et al., 2019; Peng et al., 2022). By contrast, sedimentation in proximal foreland basins is dictated by tectonic activity in the adjacent orogenic wedge, causing subsidence and uplift (see DeCelles & Giles, 1996; Peng et al., 2022). Sequence stratigraphic reconstructions in the WCSB, however, suggest that crustal flexure in response to plate coupling of the subducting plate and thrusting in the orogenic wedge propagated through the foreland basin and played a major role in the sedimentary expression of the distal foreland basin (e.g., Catuneanu, 1997; Lukie et al., 2002; Zaitlin et al., 2002; DeCelles et al., 2009).

2. Geological background

2.1. Western Canada Sedimentary Basin (WCSB)

The WCSB operated as a foreland basin during the Jurassic to Paleocene compressional phase of the Canadian Cordillera (Figure 1A–B) (Porter et al., 1982; Stockmal, 1984; Underschultz & Erdmer, 1991; Leckie & Smith, 1992; Mossop & Shetsen, 1994b; Raines et al., 2013; Pană et al., 2019; Monger & Gibson, 2019; Pană, 2021). The Canadian Cordillera is widely regarded as an accretionary orogen that developed through progressive eastward subduction of oceanic plates flooring the ancestral Pacific basin beneath the North American craton's western continental margin. Subduction is thought to have been accompanied by significant westward migration of the craton, coinciding with the opening of the central Atlantic Ocean in the Early Jurassic following the breakup of Pangea (Monger et al., 1972; Monger & Price, 2002; Monger & Gibson, 2019). Alternatively, it has been discussed that the Cordilleran orogenesis was initially driven by westward subduction that resulted in the collision of the North American craton with an archipelago of intraoceanic terranes starting in the Late Jurassic (Sigloch & Mihalynuk, 2013, 2017) or with a pre-assembled ribbon continent in the Late Cretaceous (Johnston, 2008; Hildebrand et al., 2013; Chen et al., 2019). Two main phases of significant contraction and crustal thickening are recorded in the southern Canadian Cordillera, which occurred in the Jurassic (180–160 Ma) and the late Early Cretaceous to Paleocene (~120–60 Ma) (Gehrels et al., 1991; Monger & Price, 2002; Evenchick et al., 2007; Gibson et al., 2008; Hildebrand et al., 2013; Pană & van der Pluijm, 2015; Monger & Gibson, 2019). During the Cretaceous phase of compression, the Canadian Cordillera emerged as a complete physiographic and tectonic entity similar in size and breadth as it is seen today (Monger & Gibson, 2019).

The siliciclastic Mesozoic successions of the foreland basin are underlain by Archean to Proterozoic crystalline basement, and a Paleozoic to lower Mesozoic stratigraphy that comprises mainly carbonate and evaporite successions deposited on the western margin of Laurentia (Figure 1B) (Porter et al., 1982; Frazier & Schwimmer, 1987; Leckie & Smith, 1992; Burwash et al., 1994). Paleozoic shelf and platform carbonate deposition dominated until the Triassic (540–250 Ma), and was punctuated by widespread evaporite deposition in the Middle Devonian (Aitken, 1978; Moore, 1988; Theriault, 1988; Kent, 1994; Meijer Drees, 1994; Mossop & Shetsen, 1994a; Jin & Bergman, 2001; Root et al., 2001; Buschkuehle et al., 2007; Hauck et al., 2017).

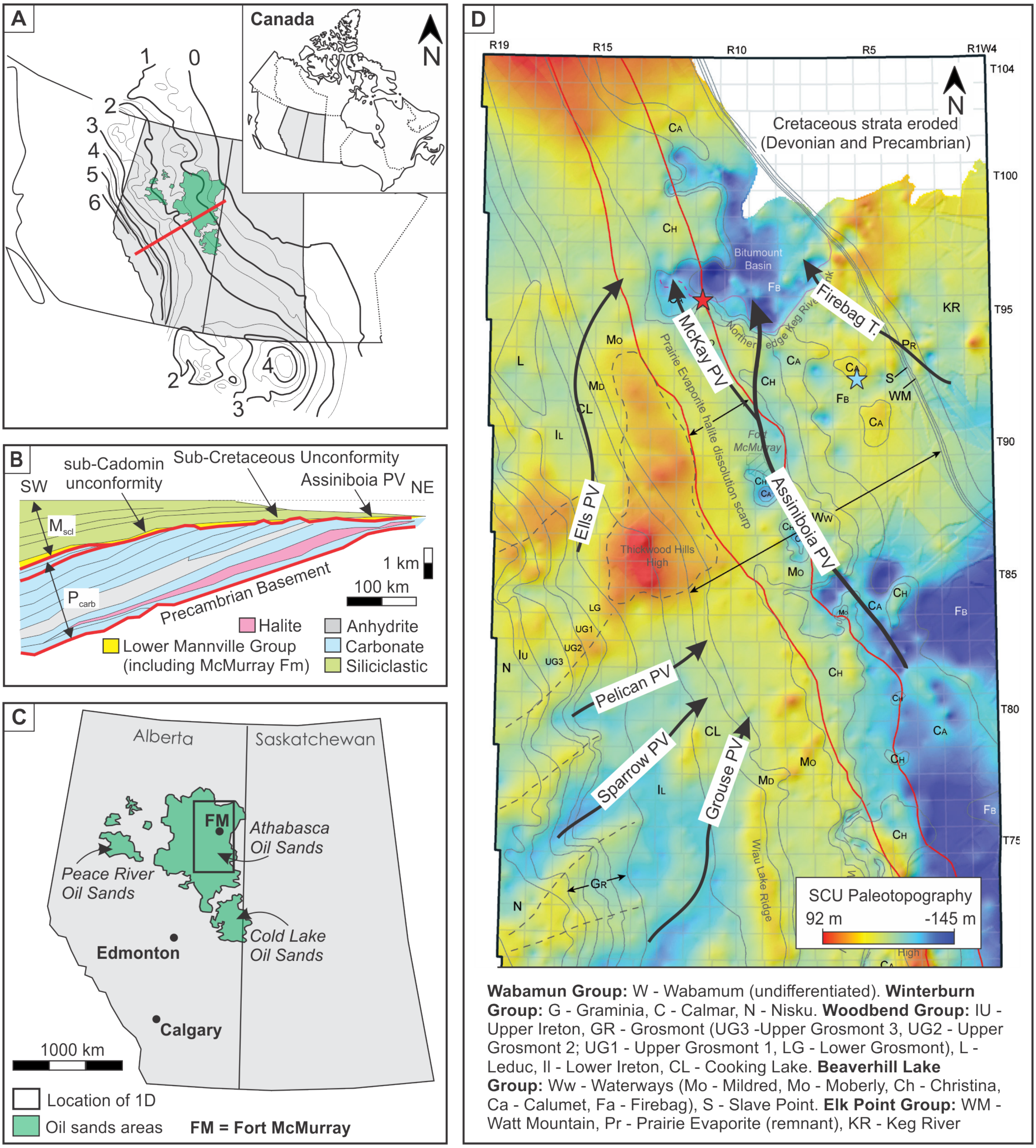

Figure 1 | Extent of the Western Canada Sedimentary Basin (WCSB) to its zero edge within western Canada (inset shows location within Canada). Isopach thicknesses (in km) of Mesozoic and younger strata in the foreland basin (A). The red line indicates the position of the cross-section displayed in (B). The green polygon displays the oil sands areas in (C) (modified after Porter et al., 1982, Ranger, 1994). (B) Schematic cross-section through the sedimentary wedge of the WCSB. Paleozoic rocks (P_{carb}) are dominated by carbonate and are truncated by the sub-Cadomin/Sub-Cretaceous Unconformity (SCU). The entire succession is tilted due to orogenic thickening to the southwest. The Mesozoic infill of the WCSB (M_{scl}) is dominated by siliciclastic strata that tapers in thickness towards the northeast. Yellow marks the lower Mannville Group, which encompasses the McMurray Formation in the distal foreland basin. The McMurray Fm is situated mainly in the Assiniboia Paleovalley (PV) and associated tributary paleovalleys. Major erosional surfaces are marked by red lines. Glacial erosion has removed much of the Mesozoic interval in the northeast (modified after Ranger, 1994). (C) Position of the Athabasca Oil Sands Region within the grey polygon in (A). The McMurray Fm hosts most of the bitumen. (D) Reconstructed paleotopography of the Sub-Cretaceous Unconformity (SCU). Inferred paleovalley-trends and flow directions (arrows) are shown. Sub-cropping stratigraphy (gray lines) and the start (west) and end (east) of the salt-dissolution scarp of the Prairie Evaporite Fm (red lines) are shown. The red star indicates the location of the sampled core lying north of the MacKay Paleovalley. The blue star indicates the sampled location for geochronology in Firebag Tributary (Rinke-Hardekopf et al., 2019). Map is modified after Hauck et al. (2017). Paleovalley positions are from Ranger (2006), Broughton (2013), and Château et al. (2019).

During the Jurassic, the WSCB was affected by flexural response to crustal loading by the emerging Canadian Cordillera (Jordan, 1981; Stockmal, 1984; Cant & Stockmal, 1989; Quinn et al., 2016; Pană et al., 2019). The Jurassic deposits accumulated in either a distal foreland or backbulge basin (see Ross et al., 2005; Fuentes et al., 2009, 2011; Miles et al., 2012; Pană et al., 2019) and are truncated by an extensive phase (~10–20 My) of erosion. The resulting angular unconformity is referred to as sub-Cadomin unconformity in the southern Canadian Cordilleran orogenic wedge and most proximal part of the foreland basin system. In the central to distal foreland basin system, the unconformity is referred to as the sub-Mannville or Sub-Cretaceous Unconformity (Pană, 2021). The formation of the widespread sub-Cadomin/ Sub-Cretaceous Unconformity is attributed to either isostatic rebound during a phase of tectonic quiescence (Cant & Stockmal, 1989; Ross et al., 2005; Miles et al., 2012) or forebulge migration combined with the effects of eustatic sea level fall (Gillespie & Heller, 1995; Fuentes et al., 2009, 2011). Barremian to Aptian sediments accumulated on the angular unconformity during the onset of overall sea level rise (Jackson, 1984; Leckie & Smith, 1992; Haq, 2014). Increased subsidence and pronounced wedge-shaped sedimentation associated with foredeep deposition are documented in the Albian (Jackson, 1984; Leckie & Smith, 1992).

Today, the sedimentary succession of the WSCB is up to 6 km thick near the orogen and tapers towards the east and northeast (Figure 1B). Mesozoic deposits encompass marine shale through to terrestrial siliciclastics (Jordan, 1981; Porter et al., 1982; Cant & Stockmal, 1989; Leckie & Smith, 1992; Pană & van der Pluijm, 2015; Quinn et al., 2016). These record deepening and shallowing cycles of the foreland basin system in response to tectonic loading and uplift in the adjacent orogenic belt to the west (Bird, 1978; Jordan, 1981; Stockmal, 1984; Underschultz & Erdmer, 1991; Fuentes et al., 2011; Raines et al., 2013; Pană et al., 2019). The deposits that accumulated in the Jurassic to Paleocene foreland basin system in the WCSB were punctuated by numerous events of erosion and/or non-deposition, caused by periods of activity in the adjacent orogenic wedge, steeping of the subducting plate, lithospheric isostatic adjustments, forebulge migration, and eustatic sea-level falls (Underschultz & Erdmer, 1991; Catuneanu et al., 1997; Price, 1994; Ross et al., 2005; Netzeband et al., 2006; Fuentes et al., 2011).

2.2. McMurray Formation

The Barremian to Aptian McMurray Fm in northeastern Alberta, Canada was deposited in the distal portion of the WCSB (i.e., distal foredeep to backbulge basins) (Figure 1A and C) (Badgley, 1952; Monger & Price, 2002; Hein et al., 2012; Pană & van der Pluijm, 2015; Monger & Gibson, 2019). Deposition of the McMurray Fm is thought to have taken place during a phase of tectonic quiescence in the Canadian orogen to the earliest onset of the Early Cretaceous to Paleocene (~120–60 Ma) phase of widespread compression in the Canadian Cordillera (see Leckie & Smith, 1992; Quinn et al., 2016). However, the position of the McMurray Fm (i.e., foredeep, forebulge, backbulge) in the evolving foreland basin system is not well constrained (e.g., Leckie & Smith, 1992; Benyon et al., 2014; Quinn et al., 2016).

The deposits of the McMurray Fm overlie the SCU (Carrigy, 1959; Mossop & Flach, 1983; Frazier & Schwimmer, 1987; Hein et al., 2012). The paleotopographic surface of the SCU resembles a series of north-south-oriented paleovalleys carved into the underlying Devonian carbonate (Carrigy, 1959; Flach & Mossop, 1985; Hein et al., 2012; Hauck et al., 2017). In the AOSR, the trunk paleovalley is referred to as the Assiniboia Paleovalley (see Christopher, 1984), into which multiple tributary paleovalleys debouched (e.g., Sparrow, Grouse and Pelican paleovalleys in the southwest, and Firebag Tributary in the east) (Figure 1D) (see Hein, 2006; Château et al., 2019).

Southward transgression of the Boreal Sea progressively filled the paleovalleys with fluvial to paralic deposits of the McMurray Fm (Carrigy, 1959; Pemberton et al., 1982; Flach & Mossop, 1985; Leckie & Smith, 1992; Ranger & Pemberton, 1997; Hein et al., 2012; Broughton, 2015; Weleschuk & Dashtgard, 2019; Château et al., 2021; Rinke-Hardekopf et al., 2022). Deposition of the McMurray occurred within an overall low-accommodation setting, but there is disagreement regarding the timing, magnitude, frequency, and cause(s) of accommodation space creation (Carrigy, 1959; Ranger & Pemberton, 1997; Hein et al., 2012; Broughton, 2015; Baniak & Kingsmith, 2018; Château et al., 2021). In the southwestern AOSR, correlation of parasequences suggests continued and step-wise retrogradation associated with transgression of the paleo-shoreline, cross-cut by autochthonous channel belts and/or allochthonous incised valleys (Figure 2) (Ranger & Pemberton, 1997; Horner et al., 2018; Château et al., 2019, 2021; Weleschuk & Dashtgard, 2019). In the southeastern AOSR, thick channel deposits are interpreted to have formed through large base-level fluctuations during overall transgression (Hein et al., 2012; Horner et al., 2019; Peng et al., 2022). In the northern AOSR, the absence of correlatable parasequences favors the application of an informal tripartite lithostratigraphic subdivision (Figure 2) (Carrigy, 1959; Keith et al., 1988; Broughton, 2015, 2018; Rinke-Hardekopf et al., 2019) wherein terrestrial deposits are assigned to the lower McMurray Fm, meandering fluvial to fluvio-tidal channel deposits comprise the middle McMurray Fm, and deltaic to brackish-water parasequences characterize the upper McMurray Fm (Carrigy, 1959).

Additional complexities derive from local to regional accommodation space variations caused by syn- and post-depositional collapse of Paleozoic strata in response to the dissolution of underlying Paleozoic carbonate and halite (Broughton, 2015, 2018; Château et al., 2019; Hein et al., 2012). In the northern AOSR, sequence stratigraphic reconstruction is further hampered by partial to complete removal of the McMurray Fm during Quaternary glaciation (Andriashek & Atkinson, 2007).

2.3. Geochronology in the Northern AOSR

Two ash beds from Firebag Tributary in northeastern AOSR were dated previously in the McMurray Fm (Table 1, Figure 1D) (Rinke-Hardekopf et al., 2019, 2022). One date is from a reworked ash layer in a coal bed in proximity to the top of the lower McMurray Fm. The other date is from a reworked ash layer in a coal bed near the top of the B1 interval, which resides in the middle part of the upper McMurray Fm (Figure 2) (Rinke-Hardekopf et al., 2019, 2022). Both samples were dated by CA-TIMS at the Isotope Geology Laboratory at Boise State University, Idaho, USA using the same procedure as in this study. The weighted mean date for the ash bed at the top of the lower McMurray Fm in Firebag Tributary is 121.39 ± 0.27 Ma (error at the 95% confidence interval) (Table 1) (after Rinke-Hardekopf et al., 2019). The MDA derived from the ash bed at the top of the B1 interval gives a weighted mean date of 115.07 ± 0.97 Ma (error at the 95% confidence interval) (after Rinke-Hardekopf et al., 2022).

2.4. Candidate magmatic sources of ash beds

Several relatively proximal (~1400–3500 km at the time; see Brown et al., 1993) magmatic sources for the ash beds of this study were active to the west, north and east of the McMurray Fm during the Aptian. Starting with more proximal sources, several magmatic events are recorded along the magmatic arc of the North American Cordillera during the Cretaceous to Paleocene. In southern Alaska, tholeitic to alkaline plutons and lavas are documented (126–105 Ma) (see Manselle et al., 2020). From northern Washington through coastal British Columbia and south-east Alaska into southwestern Yukon dioritic plutons intruded the Coast Mountain Batholith from 123–100 Ma (Gehrels, 2001; Gehrels et al., 2009). In the USA, the Peninsular Ranges Batholith and Sierra Nevada Batholith emplaced granodiorites and tonalites during 128–100 Ma and 124–105 Ma, respectively (Lackey et al., 2012; Hildebrand & Wahlden, 2018).

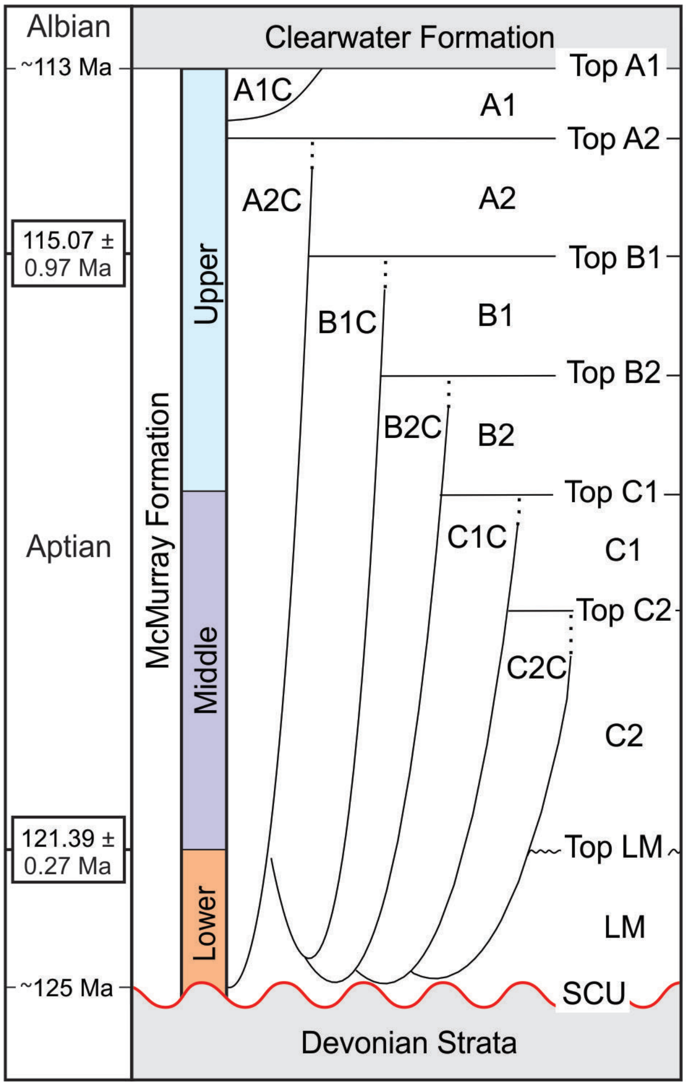

Figure 2 | Sequence stratigraphic framework developed for the McMurray Fm (right column) in the southern Athabasca Oil Sands Region (AOSR). The framework is modified after Château et al. (2021). The depositional units made of parasequence sets (A1, A2, B1, B2, C1, C2, LM) are cross-cut by autochthonous channel belts and allochthonous incised valleys (A1C, A2C, B1C, B2C, C1C, C2C). The lithostratigraphic framework commonly applied to the McMurray Fm in the Northern AOSR is shown by the colored column. The McMurray Fm overlies the Sub-Cretaceous Unconformity (SCU). Ages (left column) are provided for U-Pb dated ash beds (black boxes) at the top of the lower McMurray Fm (Top LM) and the top of B1 (with errors at the 95% confidence interval) (after Rinke-Hardekopf et al., 2019, 2022).

Farther afield, extensive igneous provinces occur in the Sverdrup basin (130–101 Ma) which was located >2500 km North of the McMurray Fm at the time (Evenchick et al., 2015; Embry & Beauchamp, 2019). These northern magmatic and volcanic events are associated with plume magmatism (Evenchick et al., 2015; Embry & Beauchamp, 2019) and predominantly tholeitic to transitional alkaline basalts (Evenchick et al., 2015).

East of the McMurray Fm, Aptian volcanic sources are located in the Scotian basin (127–118 Ma; e.g., the Orpheus Graben, Baltimore Canyon) (Pe-Piper & Piper, 2010; Bowman et al., 2012) and the New England-Quebec Igneous Province (135–114 Ma), all of which are situated >3000 km to the east in eastern Canada (e.g., Eby, 1985; Foland et al., 1989). The magmatic and volcanic activity in the Scotian basin occurred in response to plate rifting and Aptian magmatic and volcanic rocks are mildly alkalic to tholeiitic basaltic in composition (e.g., Pe-Piper et al., 1987; Pe-Piper et al. 1994; Bowman et al., 2012). The New England-Quebec Igneous Province is thought to be associated with either plume magmatism, or rifting (e.g., Eby, 1985; Boemmels et al., 2021) which emplaced Early Cretaceous alkalic to bimodal (syenite-gabbro) plutons with dominantly mafic and subordinate felsic to ultramafic dykes (McHone, 1992; Chen & Simonetti 2014).

Figure 3 | (A) Overview of the sampled core: 1AA/11-35-094-11W4. The bottom of the core is the bottom left corner and stratigraphic upsection increases towards the right. Each core column is 75 cm tall and 7 cm wide. The orange box highlights the lower McMurray Fm, and the purple box demarcates the middle McMurray Fm. The yellow box marks the interval expanded in (B). (B) Top of the lower McMurray with nine ash beds and laminae visible. Close-ups of ash layers are shown in (1)–(9). The ash beds and laminae (a) are reworked to varying degrees, and show soft-sediment deformation (s) and roots (r). The sampled ash bed occurs in (2), within a coal layer (yellow dashed box).

2.5. Sample location and regional context

The sampled ash bed is from the core of well 1AA/11-35-094-11W4, located at the northern extent of the ~45 km long, south-southeast to north-northwest trending paleovalley, herein referred to as McKay Paleovalley (Figure 1D). McKay Paleovalley is connected to the Assiniboia Paleovalley in the south and connects to the Bitumount Trough in the north (Christopher, 1984; Broughton, 2013; Hauck et al., 2017). Isopach thicknesses of the McMurray Fm in McKay Paleovalley reach up to 80 m, but vary spatially due to accommodation space variations and post-depositional glacial erosion. The McMurray Fm in the core is 33 m thick, with the lower 14.5 m interpreted as continental strata that belong to the lower McMurray. The upper 18.5 m of the core consists of inclined heterolithic stratification (IHS) and is assigned to channel deposits of the middle McMurray. Quaternary glacial erosion has removed the upper part of the McMurray Fm in the sampled core (Figure 3A). The sampled ash bed is situated at a depth of 42.73 m and is positioned within a coal seam attributed to the lower McMurray Fm. Several reworked ash beds and ash laminae are present in the coal seam (Figure 3B). The sampled ash bed is yellowish-white, convolute bedded, 0.1–2.0 cm thick, and appears to be the least reworked of all ash beds.

3. Methods

The ash sample was prepared and analyzed at the Isotope Geology Laboratory at Boise State University, Idaho, USA. Detailed description of the methods is provided in the supplementary material (S1), as well as isotopic data and resulting ages and errors (Table S1–S4, Figure S1).

3.1. Sample preparation and cathodoluminescence

The 30 g sample contains a large number (>10,000) of predominantly rounded, small (<42 ± 20 µm; probability at 0.68) zircon grains (Table S5, Figure S2). It is estimated that >99.7% of the grains are round. Forty sharply faceted grains were identified and twenty-six were sufficiently large to be mounted for cathodoluminescence (CL) imaging of internal zoning patterns (Figure 4) after annealing at 900°C for 60 hours. These grains range in length and width from 62–152 µm and 36–87 µm, respectively (Figure 4). Grain size measurements were taken from a microscope image and cathodoluminescence images (Table S5).

3.2. Geochronology

Reconnaissance U-Pb analysis using laser ablation inductively coupled plasma mass spectrometry (LA-ICPMS) was performed on the twenty-six sharply faceted zircon grains. Following LA-ICPMS analyses, U-Pb dates were obtained from seven strategically selected single zircon grains using the chemical abrasion isotope dilution thermal ionization mass spectrometry (CA-TIMS) method modified after Mattinson (2005). Grains were spiked with EARTHTIME mixed 233U-235U-205Pb tracer solution (ET535).

4. Results

LA-ICPMS on twenty-six zircon grains (<0.3% of total population) yields dates of 2,718 ± 36 Ma to 118 ± 3 Ma (errors at 2s) (Table S2). Seven zircon grains that yield Cretaceous dates (128 ± 5 Ma to 118 ± 3 Ma) were selected for CA-TIMS. The five youngest dates (< 0.05% of the initial zircon population) are equivalent with a weighted mean of 121.51 ± 0.11/ 0.11/ 0.17 Ma (Mean Squared Weighted Deviation = 0.6, probability of fit = 0.63) (Table 1): error is at the 95% confidence interval and is shown as ± x / y / z, where x is the error based on analytical uncertainties, y includes tracer calibration uncertainty, and z encompasses 238U decay constant uncertainty. One zircon returned an older date of 121.77 ± 0.11 Ma (error at 2σ), and one grain dissolved during chemical abrasion. The weighted mean date places the five youngest sharply faceted zircon in the Aptian.

5. Discussion

5.1. Depositional age of highly reworked ash

The convolute bedding of the sampled ash layer and the large proportion of rounded, detrital zircon (~99.7%) support the interpretation that the ash layer is highly reworked. Sharply faceted zircon are indicative of zircon that experienced the least bedload transport and constitute only ~0.3% of the zircon population. Such faceted zircon are most likely of primary volcanic derivation. Due to the dilution of the primary volcanic zircon population by detrital zircon and the limited number of zircon sufficiently large to be analyzed (~0.05% of the total zircon population), the CA-TIMS weighted mean of 121.51 ± 0.11 Ma from the youngest five grains is (conservatively)

Sub-basin	Lithostratigraphic position	No. of zircon	Date ± error (2σ) (Ma)	WMA ± error (95% confidence interval) (Ma)	Reference
McKay PV	Top of lower McMurray Fm	5	121.59 ± 0.21	121.51 ± 011	This study
			121.57 ± 0.31		
			121.55 ± 0.14		
			121.48 ± 0.14		
			121.41 ± 0.17		
Firebag Tributary	Top of lower McMurray Fm	5	120.99 ± 0.80	121.39 ± 0.27	After Rinke-Hardekopf et al., (2019)
			121.31 ± 0.42		
			121.23 ± 0.49		
			121.40 ± 0.53		
			121.54 ± 0.31		
Firebag Tributary	Top of B1 (middle of upper McMurray Fm)	2	115.05 ± 0.20	115.07 ± 0.97	Rinke-Hardekopf et al. (2022)
			115.11 ± 0.26		

Table 1 | Summary of zircon dates from ash beds in the McMurray Fm in McKay Palleovalley (PV; this study) and Firebag Tributary (Rinke-Hardekopf et al., 2019, 2022). Location and lithostratigraphic position within the McMurray Fm are listed. The number of zircon grains analyzed with CA-TIMS is given. Dates and weighted mean dates (WMA) have narrow error margins.

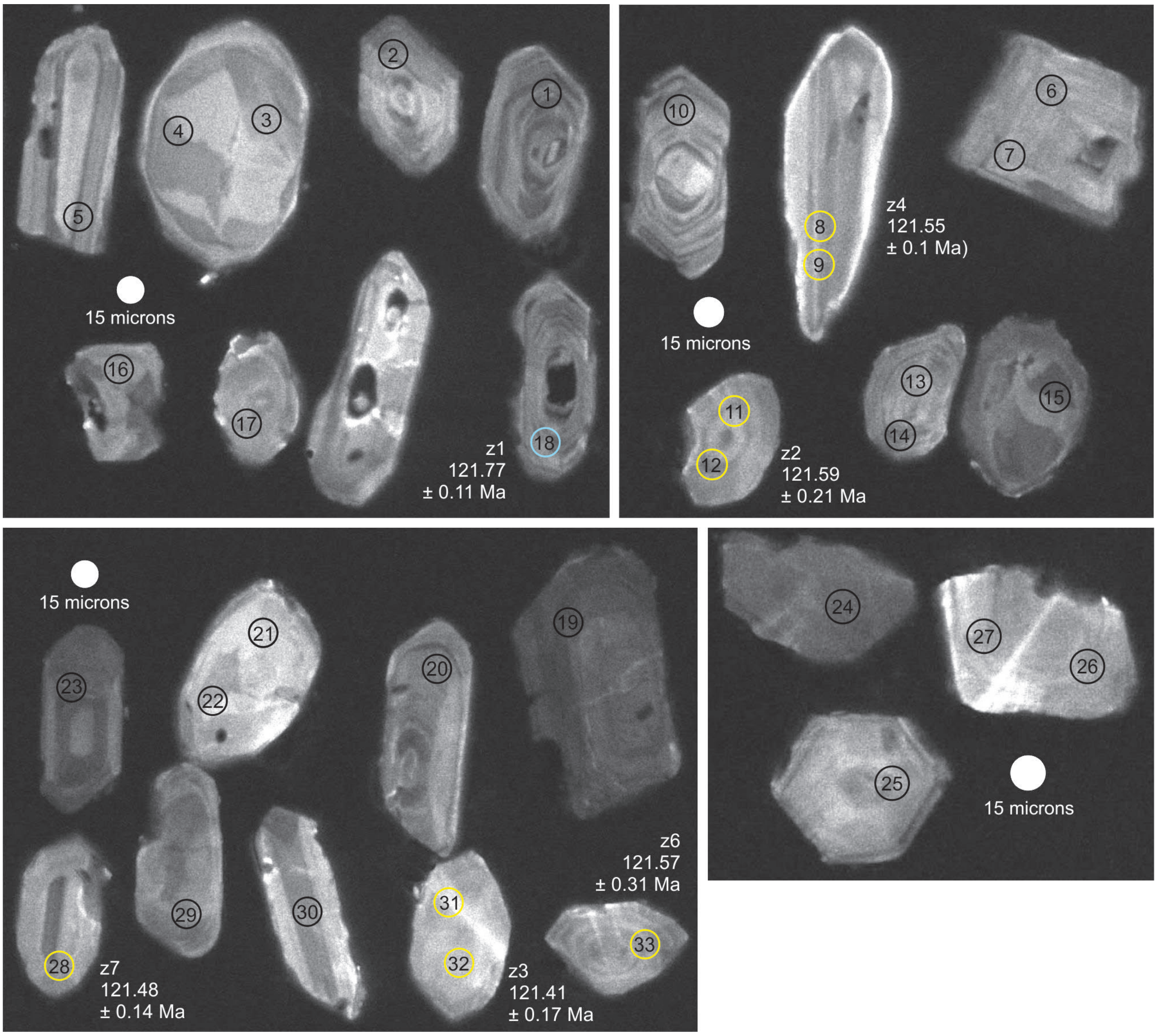

Figure 4 | Twenty-six sharply faceted zircon grains that were analyzed using LA-ICPMS. Circles demarcate the laser ablation spots. Yellow and blue circles indicate the zircon (z1–z4, z6–z7) that yielded Cretaceous LA-ICPMS dates. CA-TIMS derived dates are shown with errors at 2σ. The zircon with the blue circle was omitted from the weighted mean date calculation.

interpreted as MDA. Despite the significant reworking of the ash, the MDA is highly precise compared to previously published MDAs of reworked ash and sandstone samples in the McMurray Fm (see Benyon et al. 2014, 2016; Blum & Pecha, 2014; Quinn et al., 2018; Rinke-Hardekopf et al., 2019, 2021, 2022; Wahdi et al., 2021).

5.2. Minimal reworking and true depositional age

The ability of a MDA to represent true depositional age (TDA) is a function of geological processes (e.g., crystallization age, transport processes) and analytical methods. The very narrow age range of the five youngest zircon (Figures 5 and S1) in this study suggests they were derived from a single volcanic eruption or multiple eruptions from a single, localized source that occurred over a very short time period (~100,000 years). Catholuminescence images show no resorption surfaces indicative of inherited cores or disequilibrium with the magma during crystal growth (Figure 4), and similar host melt conditions are indicated by consistent Ti-in-zircon crystallization temperatures (T_{zircTi}, see Watson et al, 2006), Zr/Hf and Th/U values (Tables S1 and S4) (see Wang et al., 2010; Siégel et al., 2018). Previous provenance studies of the lower McMurray Fm are indicative of detrital zircon younger than 250 Ma being fluvially sourced from the Cordilleran arc in southwestern USA (e.g., Benyon et al., 2014; 2016; Blum & Pecha 2014; Wabhi et al., 2021). Deposition of the ash bed by fluvial transport is improbable. Dilution of a zircon population from a single primary source in the southwestern USA with detrital zircon to produce the sample dataset is unlikely. The small grain sizes and the sharply faceted morphology (Figure 4) support the interpretation of airborne transport. With the assumption that the crystallization age of the zircon approximates the time of volcanic eruption, or very closely spaced eruptions, the MDA (121.51 ± 0.11 Ma) is interpreted to reflect the TDA of the ash bed.

Typically, 117 randomly chosen zircon should be analyzed to calculate a robust MDA of a sample (see Vermeesch et al., 2004), which contrasts with this study's twenty-six LA-ICPMS zircon measurements. However, this study mitigates the statistical effects of random sampling by careful screening and selective targeting of zircon using

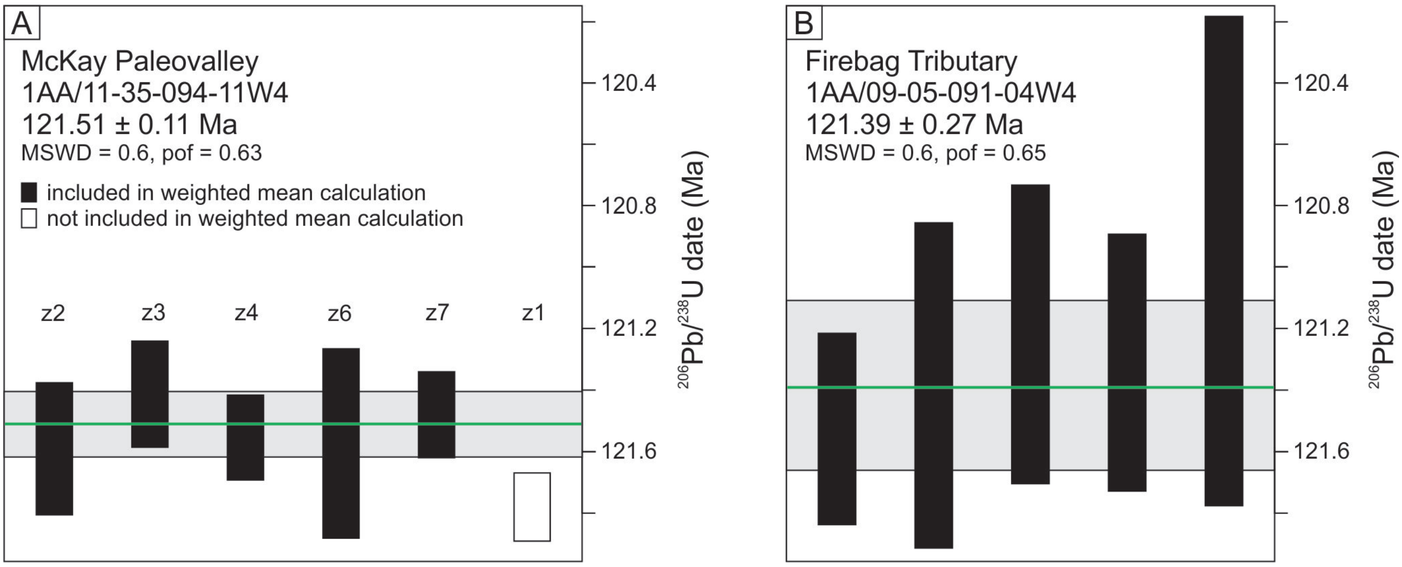

Figure 5 | CA-TIMS dates from single zircon grains from the lower McMurray Fm ash sample in A) McKay Paleovalley and B) Firebag Tributary (modified after Rinke-Hardekopf et al., 2019). Values are plotted with Isoplot 4.15 (Ludwig, 2003). Errors on individual analyses are plotted at 2σ and errors for the weighted mean dates are calculated at the 95% confidence interval. Grey boxes represent the weighted mean dates. MSWD is the mean squared weighted deviation and pof refers to the probability of fit.

visual criteria that are indicative of grains that experience minimal reworking or resorption (e.g., shape, color and size of zircon grains) (see Vermeesch et al., 2004; Sharman & Malkowski, 2020).

In a dataset of 1794 LA-ICPMS measurements of zircon from lower McMurray Fm sand, one analysis returned a younger date (116.2 ± 2.5 Ma; 0.005% of their dataset) (see Wahbi et al., 2021) than the ash bed of this study (121.51 ± 0.11 Ma). This significantly younger age is likely attributable to analytical imprecision of the LA-ICPMS method (Vermeesch 2004, 2021), or to uncertainty in the age of the sampled sand bed. CA-TIMS dates from this study overlap with those derived from a reworked ash bed in a regionally extensive coal interval at the top of the lower McMurray Fm in Firebag Tributary (Table 1) (Rinke-Hardekopf et al., 2019). The careful selection of zircon, the application of the high precision CA-TIMS dating, and the absence of younger zircon clusters in a large LA-ICPMS dataset (see Wahbi et al., 2021; Rinke-Hardekopf et al., 2022) support the interpretation of 121.51 ± 0.11 Ma as closely approximating the TDA of the ash bed. Nonetheless, it is statistically possible for a younger zircon population to remain undiscovered in the lower McMurray ash sample, or for these younger zircon to be absent (see Rossignol et al., 2019; Sharman & Malkowski, 2020).

5.3. Magmatic source of ash beds

Zircon compositions are dictated by the geochemistry of their host melt (see Belousova et al., 2002; Wang et al., 2010; Schwartz et al., 2014), which can be used to delineate potential magmatic sources. Trace element ratios derived from LA-ICPMS (e.g., Zr/Hf, Y/U) (see Tables S1 and S4) suggest a mafic to intermediate source melt (Brooks, 1970; Belousova et al., 2002) with low Th/U values (0.7–1) indicative of an intermediate source melt. The few primary zircon in the ash bed (<0.05% of zircon population) may indicate mafic to intermediate melts as a source because they produce fewer zircon than do rhyolitic melts (see Schwartz et al., 2014), although reworking of the ash bed probably contributed to the dilution primary zircon.

The mafic to intermediate signature of the zircon also suggests a source melt associated with rifting or plume activity to the north or east of the McMurray Fm. The presence of pyroclastic material in southern Alaska, the Sverdrup basin and the Scotian basin support the interpretation of a northwestern, northern or eastern source of the ash bed (see Pe-Piper & Piper, 2010; Bowman et al., 2012; Manselle et al., 2020). Despite the low magmatic flux from the western Cordillera prior to 120 Ma (see Gehrels et al. 2009), a western source of the ash bed cannot be ruled out, based on the presence of intermediate batholiths in western Canada and USA (Gehrels et al. 2009; Lackey et al., 2012; Hildebrand and Wahlden, 2014), their relative geographic proximity at the time (~1400 km) (see Brown et al. 1993), and mostly eastward-directed modeled wind patterns (see Hay & Floegel, 2012). Considering the global distribution of fine-grained pyroclastic sediment derived from large eruptions, magmatic sources at even greater distances (>3000 km) may be possible. Additional studies, including the analysis of Hf and O isotopes within the zircon are necessary in order to delineate the magmatic source of the ash bed.

5.4. Chronostratigraphy and sequence stratigraphy of the Northern AOSR

During deposition of the lower McMurray Fm, McKay Paleovalley and Firebag Tributary in the northeastern AOSR were largely disconnected geographically. McKay Paleovalley is located in the center of the northern AOSR, and was connected to, and was likely a distributary of the main Assiniboia Paleovalley system (Figure 1D). By contrast, Firebag Tributary in the northeast of the AOSR debouched into Assiniboia Paleovalley (Figure 1D).

The ash beds from McKay Paleovalley and Firebag Tributary are both located within coal seams. Like the McKay Paleovalley ash bed, it is argued that the ash bed in Firebag Tributary experienced minimal transport. These two lower McMurray ash beds also have overlapping chronostratigraphic dates (121.51 ± 0.11 Ma in McKay Paleovalley and 121.39 ± 0.27 Ma in Firebag Tributary) (Table 1). Consequently, the geochronological data from this study allows chronostratigraphic correlation of the top of the lower McMurray Fm from Firebag Tributary into McKay Paleovalley.

Ash-bearing coal seams at the top of the lower McMurray Fm have been found in several cored intervals in Firebag Tributary (Rinke-Hardekopf et al., 2019). The correlation of the ash-bearing coal seams in Firebag Tributary to those in McKay Paleovalley supports the inferred widespread extent of this mappable interval and its suitability as a key marker horizon for stratigraphic reconstructions of the northern AOSR, especially when multiple coal seams are present within one stratigraphic interval.

Moreover, a petrographic study of the lower McMurray ash-bearing coal seam in Firebag Tributary interpreted coal accumulation to have occurred in a coastal mire during the earliest onset of transgression (Rinke-Hardekopf et al., 2019). Coastal mires are hydrologically linked to sea level and basement subsidence (Flint et al., 1995; Bohacs and Suter 1997). Provided that the ash accumulated in coastal mires, the host coal beds can be regarded as having minimal paleotopographic relief regionally. Ash beds that were deposited in a near-instantaneous geological event (see previous discussion) in these near-horizontal coals seams near the top of the lower McMurray Fm may provide an alternative datum for stratigraphic cross-sections, particularly in the absence of widespread parasequence boundaries. The intraformational position of this potential datum also provides a means to delineate syn-depositional accommodation space variations for the overlying middle and upper McMurray Fm.

5.5. Record of early orogenic compression in distal foreland basins

Deposition of the McMurray Fm in the distal foreland basin system (i.e., distal foredeep, forebulge or backbulge) has led several workers to focus on large-scale, high-frequency variations in eustasy to explain the complex amalgamation of terrestrial to paralic deposits cross-cut by deeply incised channels (e.g., Hein et al., 2012; Horner et al., 2018; Peng et al., 2022). Six valley incision events are interpreted to have occurred as a product of eustatic fluctuations between 121.51–113 Ma (Figure 2) (Hein et al., 2012; Horner et al., 2018). However, during this time period, only two confirmed eustatic sea-level falls occurred (see Haq 2014; Maurer et al., 2003) and the assumption that eustasy was the primary driver of base-level changes in the McMurray Fm remains contentious (see Ranger and Pemberton, 1992; Hein et al., 2012; Broughton, 2013).

Preservation of ash beds is most probable in low-energy environments, such as mires. Several coal seams occur in the lower McMurray Fm, yet ash beds are only documented from coal seams in proximity to regional flooding surfaces (top lower McMurray and top B2) (see Rinke-Hardekopf et al., 2019, 2022). The presence of volcanic ash only in coal seams immediately prior to regional flooding surfaces suggests a linkage may exist between tectonic activity and ensuing base-level change.

The deposition of the Barremian to Aptian McMurray Fm occurred just prior to and during the early onset of the Early Cretaceous to Paleocene phase (~120–80 Ma) of significant compression in the Canadian Cordillera (e.g., Leckie & Smith 1992; Pană and Pluijm, 2015; Monger and Gibson 2019). The sheet-like geometry of Aptian strata in the WCSB (Jackson 1984; Leckie & Smith 1992) has been argued to reflect deposition prior to significant orogenic compression and foreland basin development. Nonetheless, tectonic activity in the southern Canadian Cordillera occurred during the deposition of the McMurray Fm, including thrust activation of the Southern Rocky Mountain Trench (136–110 Ma) and deformation east of the Kootenay Arc (143–111 Ma) and northern Monashee-southern Cariboo mountains (136–122 Ma) (Currie, 1988; Crowley et al., 2000; Gibson et al., 2005, 2008; Moynihan & Pattison, 2013; Webster et al., 2014; Pană et al., 2019). Contemporaneously, Barremian to Aptian widespread magmatism associated with rifting occurred along the Scotian basin and possibly the New England-Quebec Igneous Province (130–110 Ma) east of the McMurray Fm (see Pe-Piper et al., 2010; Boemmels et al., 2021). This Early Cretaceous tectonic activity coincides with lithospheric uplift and the formation of the Sub-Cretaceous Unconformity (Cant and Stockmal 1989; Gillespie and Heller, 1995; Ross et al., 2005; Fuentes et al., 2009, 2011; Miles et al., 2012), as well as eastward-directed fluid flux through sediments in the foreland basin (125 –115 Ma) ("tectonic squeegee" after Oliver, 1986 or "hot fluid flush" after Pană et al., 2019), which may have enhanced salt dissolution of the Prairie evaporite underlying the McMurray Fm. These Early Cretaceous tectonic events occurred prior to pronounced foreland basin development in the Albian, but are likely to have influenced Aptian strata in the WCSB.

Tectonic activity propagates through the lithosphere and in the WCSB, it has been found to play a major role in high-frequency variations in both proximal and distal foreland basin sedimentation (e.g., Catuneanu, 1997; Lukie et al., 2002; Yoshida et al., 2000; Zaitlin et al., 2002; DeCelles, 2004). The frequency of tectonically induced incision events in the foreland basin system of the Canadian Cordillera is reported on scales similar to those seen in the McMurray Fm (e.g., Catuneanu, 1997; Lukie et al., 2002; Yoshida

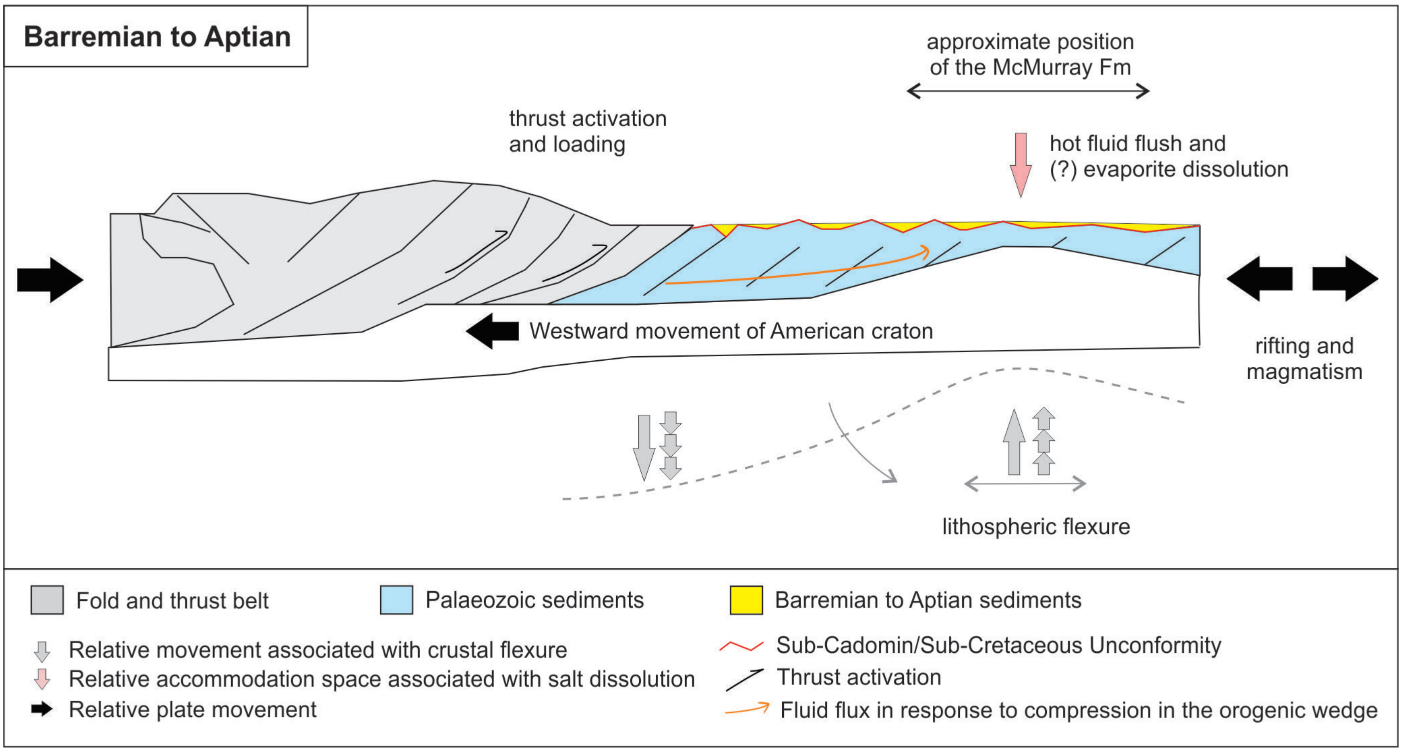

Figure 6 | Schematic representation of the tectonic setting of the McMurray Fm during the Barremian to Aptian. Onset of shortening in the foreland basin system was accompanied with renewed activation of thrusts in the orogenic wedge of the southern Canadian Cordillera, fluid flush towards the distal foreland basin system, and flexural steepening accompanied with uplift of the forebulge and rifting in the east and north of the McMurray Fm (modified after Pană et al., 2019).

et al., 2000; Zaitlin et al., 2002). In fact, accommodation space variations in the Barremian to Aptian Basal Quartz Formation in southern Alberta are attributed to regional tectonic processes (Ardies et al., 2002; Lukie et al., 2002; Zaitlin et al., 2002).

It is plausible that dynamic processes in the mantle produced by the shortening of the foreland basin system, and vertical and lateral displacement of the forebulge (see Pană et al., 2019, 2021), as well as enhanced plate coupling of the North American craton with the subducting oceanic plate contributed to the high-frequency fluctuations in accommodation space that are observed farther afield within the McMurray Fm of the AOSR (Figure 6). The large sediment supply from the inferred continental-scale paleodrainage system (see Blum and Pecha, 2014) to the low-accommodation space basin may have contributed to the rapid fill following phases of lithospherically induced uplift during overall sea level rise.

6. Conclusions

Careful analytical treatment of a reworked ash bed in the lower McMurray Fm of McKay Paleovalley returned highly precise and accurate zircon dates with a weighted mean of 121.51 ± 0.11 Ma, which is conservatively considered a robust MDA and likely represents a true depositional age. The date agrees with the previously published MDA (121.39 ± 0.27 Ma) for the coal interval near the top of the lower McMurray Fm in Firebag Tributary and places the top of the lower McMurray Fm firmly in the Aptian.

This is only the second date for the lower McMurray Fm, but it allows a chronostratigraphic assessment of the earliest infill in the northern AOSR. The dates establish a chronostratigraphic surface that allows correlation of McKay Paleovalley strata with similar age strata in Firebag Tributary. The ash-bearing coal seams at the top of the lower McMurray Fm form a key marker bed of widespread extent that marks a previously interpreted flooding surface and onset of transgression. Consequently, the coal-bearing interval at the top of the lower McMurray Fm is a regional marker bed that can be used for basin-wide correlation of strata.

The ash beds in the lower McMurray Fm coal seams also have the potential to act as an intraformational datum, which may aid in the assessment of syn-depositional accommodation space variations. Further, the occurrence of the ash beds below a significant flooding surface in the AOSR suggests that tectonic activity during the onset of the Early Cretaceous emergence of the Canadian Cordillera influenced accommodation space variations in the distal parts of the adjacent foreland basin.

Acknowledgments

This research was supported by BP Canada Energy Group ULC, Cenovus Energy Incorporation, Husky Energy Incorporation (now part of Husky Energy Group ULC), Nexen (now part of CNOOC International Ltd), and Woodside Petroleum Ltd (now part of Woodside Energy Group Ltd). Funding was also received from a Natural Sciences and Engineering Research Council of Canada (NSERC) Discovery Grant awarded to JAM. The authors thank Mike Ranger for his logistical support. Glyn Williams-Jones is thanked for input regarding the assessment of ash bed magmatic sources. Steve Hubbard and Brent C. Ward provided helpful comments associated with an earlier version of this manuscript. The authors thank the editor Dr. S. Bodin and the associate editor Dr. J. Bailleul. The paper benefited from the helpful reviews that were received from Dr. D.I. Pană, Dr. L. Caracciolo and Dr. M. Roddaz.

Authors contribution

Conceptualization: S.W. Fietz, J.L. Crowley, J.A. MacEachern, S.E. Dashtgard and H. D. Gibson. Material collection: S.W. Fietz. Laboratory analyzes: J.L. Crowley. Organisation: S.W. Fietz. Original draft : S.W. Fietz and J.L. Crowley. Art design : S.W. Fietz and J.L. Crowley. Funding acquisition: J.A. MacEachern. Revision: J.L. Crowley, J.A. MacEachern, S.E. Dashtgard and H. D. Gibson. Supervision: J.L. Crowley, J.A. MacEachern, S.E. Dashtgard and H. D. Gibson. All authors have read and agreed to the submitted version of the manuscript.

Data availability

All data of this study are free-to-use and openly available in the supplementary materials of this study. The sampled core 1AA/11-35-094-11W4 is publicly available at the Core Research Centre in Calgary, Alberta, Canada.

Conflict of interest

We have no conflict of interest to disclose.

Supplementary items

Supplementary data comprise an extended description of the methods (S1), five tables (Table S1–S5) and two figures (Figures S1 and S2). Tables S1–S3 are grouped into one Excel file and describe LA-ICPMS instrumental data, U-Pb isotopic and trace element data of the analyzed zircon, and standard data. Table S4 contains the CA-TIMS U-Pb isotopic data and calculated weighted mean date. Table S5 and Figure S2 describe the appearance of zircon and are both provided in one Excel file. Table S5 contains data on grain size measurements from 335 zircon grains. Detrital zircon grains were measured from Figure S2 and from cathodoluminescence images (Figure 4). Figure S1 displays the Concordia plot of CA-TIMS U-Pb dates.

References

Aitken, J. D. (1978). Revised models for depositional Grand Cycles, Cambrian of the southern Rocky Mountains, Canada. Bulletin of Canadian Petroleum Geology, 26, 515–542. https://doi.org/10.35767/gscpgbull.26.4.515

Ardies, G. W., Dalrymple, R. W., & Zaitlin, B. A. (2002). Controls on the geometry of incised valleys in the Basal Quartz unit (Lower Cretaceous), Western Canada Sedimentary Basin. Journal of Sedimentary Research, 72, 602–618. https://doi.org/10.1306/032101720602

Andriashek, L. D., & Atkinson, N. (2007). Buried channels and glacial-drift aquifers in the Fort McMurray region, northeast Alberta (EUB/AGS Earth Sciences Report 2007-01). Energy and Utilities Board.

Baadsgaard, H., & Lerbekmo, J. F. (1983). Rb-Sr and U-PB dating of bentonites. Canadian Journal of Earth Sciences, 20, 1283–1290. https://doi.org/10.1139/e83-113

Badgley, P. C. (1952). Notes on the subsurface stratigraphy and oil and gas geology of the Lower Cretaceous series in central Alberta. Geological Survey of Canada Paper, 52-11, 1–12.

Baniak, G. M., & Kingsmith, K. G. (2018). Sedimentological and stratigraphic characterization of Cretaceous upper McMurray deposits in the southern Athabasca oil sands, Alberta, Canada. American Association of Petroleum Geologists Bulletin, 102, 309–332. https://doi.org/10.1306/0502171619317010

Belousova, E. A., Griffin, W. L., O'Reilly, S. Y., & Fisher, N. I. (2002). Igneous zircon. Trace element composition as an indicator of source rock type. Contributions to Mineralogy and Petrology, 143, 602–622. https://doi.org/10.1007/s00410-002-0364-7

Benyon, C., Leier, A. L., Leckie, D. A., Hubbard, S. M., & Gehrels, G. E. (2016). Sandstone provenance and insights into the paleogeography of the McMurray Formation from detrital zircon geochronology, Athabasca Oil Sands, Canada. American Association of Petroleum Geologists Bulletin, 100, 269–287, https://doi.org/10.1306/10191515029

Benyon, C., Leier, A., Leckie, D. A., Webb, A., Hubbard, S. M., & Gehrels, G. (2014). Provenance of the Cretaceous Athabasca Oil Sands, Canada: Implications for Continental-Scale Sediment Transport. Journal of Sedimentary Research, 84, 136–143. https://doi.org/10.2110/jsr.2014.16

Bhattacharya, J. P. (2011). Practical problems in the application of the sequence stratigraphic method and key surfaces: integrating observations from ancient fluvial-deltaic wedges with Quaternary and modelling studies. Sedimentology, 58, 120–169. https://doi.org/10.1111/j.1365-3091.2010.01205

Bhattacharya, J. P., & Willis, B. J. (2001). Lowstand deltas in the Frontier Formation, Powder River basin, Wyoming: Implications for sequence stratigraphic models. American Association of Petroleum Geologists Bulletin, 85, 261–294. https://doi.org/10.1306/8626C7B7-173B-11D7-8645000102C1865D

Bird, P. (1978). Finite elements modeling of lithosphere deformation: the Zagros collision orogeny. Tectonophysics, 50, 307–336. https://doi.org/10.1016/0040-1951(78)90140-3

Blum, M., & Pecha, M. (2014). Mid-cretaceous to paleocene North American drainage reorganization from detrital zircons. Geology, 42, 607–610. https://doi.org/10.1130/G35513.1

Bohacs, K., & Suter, J. (1997). Sequence stratigraphic distribution of coaly rocks: Fundamental controls and paralic examples. American Association of Petroleum Geologists Bulletin, 81, 1612–1639. https://doi.org/10.1306/7834e192-1721-11d7-8645000102c1865d

Boltwood, B. (1907). Ultimate disintegration products of the radio-active elements, Part II: disintegration products of Uranium. American Journal of Science, 23, 77–88. https://doi.org/10.2475/AJS.S4-23.134.78

Boemmels, J. R. C., Crespi, J. M., Webb, L. E., & Fosdick, J. C. (2021). Ar/Ar and LA-ICP-MS U-Pb geochronology for the New England portion of the Early Cretaceous New England-Quebec igneous province: Implications for the postrift evolution of the eastern North American Margin. American Journal of Science, 321, 365–391. https://doi.org/10.2475/03.2021.03

Bowman, S. J., Pe-Piper, G., Piper, D. J. W., Fensome, R. A., & King, E. L. (2012). Early Cretaceous volcanism in the Scotian basin. Canadian Journal of Earth Sciences, 49, 1523–1539. https://doi.org/10.1139/e2012-063

Brooks, C. (1970). The concentrations of zirconium and hafnium in some igneous and metamorphic rocks and minerals. Geochimica et Cosmochimica Acta, 34, 411–416.

Broughton, P. L. (2013). Devonian salt dissolution-collapse breccias flooring the Cretaceous Athabasca oil sands deposit and development of lower McMurray Formation sinkholes, northern Alberta Basin, Western Canada. Sedimentary Geology, 283, 57–82. https://doi.org/10.1016/j.sedgeo.2012.11.004.

Broughton, P. L. (2015). Syndepositional architecture of the northern Athabasca oil sands deposit, northeastern Alberta. Canadian Journal of Earth Sciences, 52, 21–50. https://doi.org/10.1139/cjes-2014-0021

Broughton, P. L. (2018). Orogeny and the collapse of the Devonian Prairie Evaporite karst in western Canada: impact on the overlying Cretaceous Athabasca Oil Sands. In M. Parise, F. Gabrovsek, G. Kaufmann, and N. Ravbar (Eds.), Advances in Karst Research: Theory, Fieldwork and Applications (Special Publications 466, pp. 25–78): Geological Society of London. https://doi.org/10.1144/SP466.7

Brown, R. L., Beaumont, C., & Willett, S. D. (1993). Comparison of the Selkirk fan structure with mechanical models: Implications for interpretation of the southern Canadian Cordillera. Geology, 21, 1015–1018. https://doi.org/10.1130/0091-7613(1993)021<1015:COTSFS>2.3.CO;2

Burwash, R. A., McGregor, C. R., & Wilson, J. A. (1994). Precambrian basement beneath the Western Canada Sedimentary Basin. In G. Mossop, and I. Shetsen (Eds.), Atlas of the Western Canada Sedimentary Basin (pp. 49–56): Canadian Society of Petroleum Geology and Alberta Research Council. https://ags.aer.ca/reports/atlas-western-canada-sedimentary-basin

Buschkuehle, B. E., Hein, F. J., & Grobe, M. (2007). An overview of the geology of the Upper Devonian Grosmont carbonate bitumen deposit, northern Alberta, Canada. Natural Resources Research, 16, 3–15. https://doi.org/10.1007/s11053-007-9032-y

Cant, D. J., & Stockmal, G. S. (1989). The Alberta foreland basin: relationship between stratigraphy and Cordilleran terrane-accretion events. Canada Journal of Earth Sciences, 26, 1964–1975. https://doi.org/10.1139/e89-166

Carrigy, M. A. (1959). Geology of the McMurray Formation, Part III: General Geology of the McMurray Area. Alberta Geological Survey.

Catuneanu, O., Sweet, A. R., & Miall, A. D. (1997). Reciprocal architecture of Bearpaw T-R sequences, uppermost Cretaceous, Western Canada Sedimentary Basin. Bulletin of Canadian Petroleum Geology, 45, 675–694. https://doi.org/10.35767/gscpgbull.45.1.075

Château, C. C. F., Dashtgard, S. E., MacEachern, J. A., & Hauck, T. E. (2019). Parasequence architecture in a low-accommodation setting, impact of syndepositional carbonate epikarstification, McMurray Formation, Alberta, Canada. Marine and Petroleum Geology, 104, 168–179. https://doi.org/10.1016/j.marpetgeo.2019.03.021

Château, C. C. F., Dashtgard, S. E., & MacEachern, J. A. (2021). Acceleration in the rate of the Boreal Sea transgression recorded in the Lower Cretaceous McMurray Formation, Canada. Marine and Petroleum Geology, 133, 105221. https://doi.org/10.1016/j.marpetgeo.2021.105221

Christopher, J. E. (1984). The Lower Cretaceous Mannville Group, northern Williston Basin region, Canada. In D. F. Stott, and D. J. Glass (Eds.), The Mesozoic of Middle North America (pp. 109–126): Canadian Society of Petroleum Geologists.

Chen, Y., Gu, Y. J. C., Claire A., Johnston, S. T., Hung, S.-H., Schaeffer, A. J., & Audet, P. (2019). Seismic evidence for a mantle suture and implications for the origin of the Canadian Cordillera. Nature Communications, 10, 2249. https://doi.org/10.1038/s41467-019-09804-8

Chen, Y., & Simonetti, A. (2014). Evidence for the multi-stage petrogenetic history of the Oka Carbonatite Complex (Québec, Canada) as recorded by perovskite and apatite. Minerals, 4, 437–476. https://doi.org/10.3390/min4020437

Cohen, K., Finney, S. C., Gibbard, P. L., & Fan, J.-X. (2013). The ICS International Chronostratigraphic Chart. Episodes, 36, 199–204. https://doi.org/10.18814/epiiugs/2013/v36i3/002

Condon, D. J., Schoene, B., Mclean, N. M., Bowring, S. A., & Parrish, R. R. (2015). Metrology and traceability of U-Pb isotope dilution geochronology (EARTHTIME tracer calibration part I). Geochimica et Cosmochimica Acta, 164, 464–480. https://doi.org/10.1016/j.gca.2015.05.026

Crowley, J. L., Ghent, E. D., Carr, S. D., Simony, P. S., & Hamilton, M. A. (2000). Multiple thermotectonic events in a continuous metamorphic sequence, Mica Creek area, southeastern Canadian Cordillera. Geological Materials Research, 2, 1–45.

Currie, L. D. (1988). Geology of the Allan Creek area, Cariboo Mountains, British Columbia [M.Sc. thesis]. University of Calgary, Calgary. https://prism.ucalgary.ca. https://doi.org/10.11575/PRISM/19067

DeCelles, P. (2012). Foreland basin systems revisited: variations in response to tectonic settings. In C. Busby, and A. Azor, A. (Eds.), Tectonics of Sedimentary Basins: Recent Advances (pp. 405–426): Blackwell Publishing Ltd. https://doi.org/10.1002/9781444347166.ch20

DeCelles, P. G., & Giles, K. A. (1996). Foreland basin systems. Basin Research, 8, 105–123. https://doi.org/10.1046/j.1365-2117.1996.01491.x

DeCelles, G. (2004). Late Jurassic to Eocene evolution of the Cordilleran thrust belt and foreland basin system, western U.S.A. American Journal of Science 304, 105–168. https://doi.org/10.2475/ajs.304.2.105

DeCelles, G., Ducea, M. N., Kapp, P., & Zandt, G. (2009). Cyclicity in Cordilleran orogenic systems. Nature Geoscience, 2, 251–257, https://doi.org/10.1038/ngeo469

Eby, G. N. (1985). Age relations, chemistry, and petrogenesis of mafic alkaline dikes from the Monteregian Hills and younger White Mountain igneous provinces. Canadian Journal of Earth Sciences, 22, 1103–1111. https://doi.org/10.1139/e85-112

Embry A., & Beauchamp, B. (2019). Sverdrup basin. In A. Miall (Ed.), The Sedimentary Basins of the United States and Canada (pp. 559–592): Elsevier B.V. https://doi.org/10.1016/B978-0-444-63895-3.00014-0

Evenchick, C. A., Davis, W. J., Bédard, J. H., Hayward, N., & Friedman, R. M. (2015). Evidence for protracted High Arctic large igneous province magmatism in the central Sverdrup Basin from stratigraphy, geochronology, and paleodepths of saucer-shaped sills. Bulletin of the Geological Society of America, 127, 1366–1390. https://doi.org/10.1130/B31190.1

Evenchick, C. A., McMechan, M. E., McNicoll, V. J., & Carr, S. D. (2007). A synthesis of the Jurassic - Cretaceous tectonic evolution of the central and southeastern Canadian Cordillera: exploring links across the orogen. In J. W. Sears, T. A. Harms, and C. A. Evenchick, C. A. (Eds.), Whence the Mountains? Inquiries into the Evolution of Orogenic Systems: A Volume in Honor of Raymond A. Price (pp. 117–145): Geological Society of America. https://doi.org/10.1130/2007.2433(06)

Flach, P. D., & Mossop, G. D. (1985). Depositional environments of Lower Cretaceous McMurray Formation, Athabasca oil sands, Alberta. American Association of Petroleum Geologists Bulletin, 69, 1195–1207. https://doi.org/10.1306/AD462BAF-16F7-11D7-8645000102C1865D

Flint, S., Aitken, J., & Hampson, G. (1995). Application of sequence stratigraphy to coal-bearing coastal plain successions: Implications for the UK Coal Measures (Special Publication 82). Geological Society. https://doi.org/10.1144/GSL.SP.1995.082.01.01

Foland, K. A., Chen, J. F., Linder, J. S., Henderson, C. M. B., & Whillans, I. M. (1989). High-resolution 40Ar/39Ar chronology of multiple intrusion igneous complexes - Application to the Cretaceous Mount Brome complex, Quebec, Canada. Contributions to Mineralogy and Petrology, 102, 127–137. https://doi.org/10.1007/BF00375335

Frazier, W. J., & Schwimmer, D. R. (1987). Regional stratigraphy of North America. Plenum Press, 719 pp. https://doi.org/10.1007/978-1-4613-1795-1

Fuentes, F., DeCelles, P. G., Constenius, K. N., & Gehrels, G. E. (2011). Evolution of the Cordilleran foreland basin system in northwestern Montana, U.S.A. Bulletin of the Geological Society of America, 123, 507–533. https://doi.org/10.1130/B30204.1

Fuentes, F., DeCelles, P. G., & Gehrels, G. E. (2009). Jurassic onset of foreland basin deposition in northwestern Montana, USA: Implications for along-strike synchroneity of Cordilleran orogenic activity. Geology, 37, 379–382. https://doi.org/10.1130/G25557A.1

Gehrels, G. E. (2001). Geology of the Chatham Sound region, southeast Alaska and coastal British Columbia. Canadian Journal of Earth Sciences, 38, 1579–1599. https://doi.org/10.1139/cjes-38-11-1579

Gehrels, G. E., McClelland, W. C., Samson, S. D., Patchett, P. J., & Brew, D. A. (1991). U-Pb geochronology of Late Cretaceous and early Tertiary plutons in the northern Coast Mountains batholith. Canadian Journal of Earth Sciences, 28, 899–911. https://doi.org/10.1139/e91-082

Gehrels, G. E., Rusmore, M., Woodsworth, G., Crawford, M., Andronicos, C., Hollister, L., Patchett, J., Ducea, M., Butler, R., Klepeis, K., Davidson, C., Friedman, R., Haggart, J., Mahoney, B., Crawford, W., Pearson, D., & Girardi, J. (2009). U-Th-Pb geochronology of the Coast Mountains batholith in north-coastal British Columbia: Constraints on age and tectonic evolution. Bulletin of the Geological Society of America, 121, 1341–1361. https://doi.org/10.1130/B26404.1

Gibson, H. D., Brown, R. L., & Carr, S. D. (2005). U-Th-Pb geochronologic constraints on the structural evoluiton of the Selkirk fan, northern Selkirk Mountains, southern Canadian Cordillera. Journal of Structural Geology, 27, 1899–1924. https://doi.org/10.1016/j.jsg.2005.05.014

Gibson, H. D., Brown, R. L., & Carr, S. D. (2008). Tectonic evolution of the Selkirk fan, southeastern Canadian Cordillera: a composite Middle Jurassic - Cretaceous orogenic structure. Tectonics, 27, 1–14. https://doi.org/10.1029/2007TC002160.

Gillespie, J. M., & Heller, L. (1995). Beginning of foreland subsidence in the Columbian-Sevier belts, southern Canada and northwest Montana. Geology, 23, 723–726. https://doi.org/10.1130/0091-7613(1995)023<0723:BOFSIT>2.3.CO;2

Haq, B. U. (2014). Cretaceous eustasy revisited. Global and Planetary Change, 113, 44–58. https://doi.org/10.1016/j.gloplacha.2013.12.007

Hauck, T. E., Peterson, J. T., Hathway, B., Grobe, M., & MacCormack, K. (2017). New insights from regional-scale mapping and modelling of the Paleozoic succession in northeast Alberta: paleogeography, evaporite dissolution, and controls on Cretaceous depositional patterns on the sub-Cretaceous unconformity. Bulletin of Canadian Petroleum Geology, 65, 87–114. https://doi.org/10.2113/gscpgbull.65.1.87

Hay, W. W., & Floegel, S. (2012). New thoughts about the Cretaceous climate and oceans. Earth-Science Reviews, 115, 262–272. https://doi.org/10.1016/j.earscirev.2012.09.008

Hein, F. (2006). Subsurface geology and facies characterization of the Athabasca Wabiskaw-McMurray succession in the Lewis and Firebag-Sunrise areas, northeastern Alberta. In C. F. Gilboy and S. G. Whittaker (Eds.), Saskatchewan and Northern Plains Oil & Gas Symposium 2006 (pp. 238–248): Saskatchewan Geological Society.

Hein, F. J., Fairgrieve, B., & Dolby, G. (2012). A regional geologic framework for the Athabasca oil sands, northeastern Alberta, Canada. In F. J. Hein, D. Leckie, S. Larter, and J. R. Suter (Eds.), Heavy-oil and Oil-sand Petroleum Systems in Alberta and Beyond (Vol. 64, pp. 207–250): American Association of Petroleum Geologists. https://doi.org/10.1306/13371581St643550

Hildebrand, R. S. (2013). Mesozoic Assembly of the North American Cordillera (Special Paper 495, 169 pp). Geological Society of America. https://doi.org/10.1130/2013.2495

Hildebrand R. S., & Wahlden, J. B. (2018). The Tectonic Setting and Origin of Cretaceous Batholiths within the North American Cordillera: The Case for Slab Failure Magmatism and Its Significance for Crustal Growth (Special Papers, 532, 113 pp). Geological Society of America. https://doi.org/10.1130/2017.2532

Horner, S. C., Hubbard, S. M., Martin, H. K., & Hagstrom, C. A. (2019). Deducing Aptian drainage evolution with regional subsurface mapping and channel-bar scaling, western Canada foreland basin. Sedimentary Geology, 385, 26–44. https://doi.org/10.1016/j.sedgeo.2019.03.012

Horner, S. C., Hubbard, S. M., Martin, H. K., Hagstrom, C. A., & Leckie, D. A. (2018). The impact of Aptian glacio-eustasy on the stratigraphic architecture of the Athabasca oil sands, Alberta, Canada. Sedimentology, 66, 1600–1642. https://doi.org/10.1111/sed.12545

Huff, W. D. (2016). K-bentonites: a review. American Mineralogist, 101, 43–70. https://doi.org/10.2138/am-2016-5339

Jackson, R. G. (1984). Depositional model of point bars in the lower Wabash River. Journal of Sedimentary Petrology, 46, 579–594. https://doi.org/10.1306/212F6FF5-2B24-11D7-8648000102C1865D

Jin, J., & Bergman, K. M. (2001). Revised stratigraphy of the Middle Devonian (Givetian) Winnipegosis carbonate-Prairie Evaporite transition, Elk Point Group, southern Saskatchewan. Bulletin of Canadian Petroleum Geology, 49, 441–457. https://doi.org/10.2113/49.4.441

Johnston, S. T. (2008). The Cordilleran ribbon continent of North America. Annual Review of Earth and Planetary Sciences, 36, 495–530. https://doi.org/10.1146/annurev.earth.36.031207.124331

Jordan, T. E. (1981). Thrust loads and foreland basin evolution Cretaceous, western United States. American Association of

Petroleum Geologists Bulletin, 65, 2506–2520. https://doi.org/10.1306/03B599F4-16D1-11D7-8645000102C1865D

Keith, D. A. W., Wightman, D. M., Pemberton, S. G., MacGillivray, J. R., Bereznuik, T., & Berhane, H. (1988). Sedimentoloy of the McMurray Formation and Wabiskaw Member (Clearwater Formation), Lower Cretaceous, in the central region of the Athabasca oil sands area, northeastern Alberta. In D. P. James and D. A. Leckie (Eds.), Sequences, Stratigraphy, Sedimentology: Surface and Subsurface (pp. 309–324): Canadian Society of Petroleum Geologists. https://doi.org/10.1016/j.marpetgeo.2022.105775

Kent, D. M. (1994). Paleogeographic evolution of the cratonic platform - Cambrian to Triassic. In G. Mossop, and I. Shetsen (Eds.), Atlas of the Western Canada Sedimentary Basin (pp. 69–86): Canadian Society of Petroleum Geology and Albtera Research Council. https://ags.aer.ca/reports/atlas-western-canada-sedimentary-basin

Lackey, J. S., Robinson C. M., Windham C. J., Frazer, R. E., Bindeman, I. N., & Gehrels, G. E. (2012). The fine gold intrusive suite: The roles of basement terranes and magma source development in the Early Cretaceous Sierra Nevada batholith. Geosphere, 8, 292–313. https://doi.org/10.1130/GES00745.1

Leckie, D. A., & Smith, D. G. (1992). Regional setting, evolution, and depositional cycles of the western Canada foreland basin. In R. W. Macqueen and D. A. Leckie (Eds.), Foreland Basins and Fold Belts (pp. 9–46): American Association of Petroleum Geologists Bulletin. https://doi.org/10.1306/M55563C2

Lin, W., Bhattacharya, J. P., & Stockford, A. (2019). High-resolution sequence stratigraphy and implications for Cretaceous glacio-eustasy of the Late Cretaceous Gallup system, New Mexico, USA. Journal of Sedimentary Research, 89, 552–575. https://doi.org/10.2110/jsr.2019.32

Lukie, T. D., Ardies, G. W., Dalrymple, R. W., & Zaitlin, B. A. (2002). Alluvial architecture of the Horsefly unit (Basal Quartz) in southern Alberta and northern Montana: influence of accommodation changes and comtemporaneous faulting. Bulletin of Canadian Peroleum Geology, 50, 73–91. https://doi.org/10.2113/50.1.73

Ludwig, K. R. (2003). User's Manual for Isoplot 3.00. Berkeley, CA, Berkeley Geochronology Center.

Manselle, P., Brueseke, M. E., Trop, J. M., Benowitz, J. A., Snyder, D. C., & Hart, W. K. (2020). Geochemical and stratigraphic Analysis of the Chisana Formation, Wrangellia Terrane, eastern Alaska: insights into Early Cretaceous magmatism and tectonics along the northern Cordilleran margin. Tectonics, 39, 1–23. https://doi.org/10.1029/2020TC006131

Mattinson, J. M. (2005). Zircon U–Pb chemical abrasion ("CA-TIMS") method: combined annealing and multi-step partial dissolution analysis for improved precision and accuracy of zircon ages. Chemical Geology, 220, 47–66. https://doi.org/10.1016/j.chemgeo.2005.03.011

Mattinson, J. M. (2010). Analysis of the relative decay constants of 235U and 238U by multi-step CA-TIMS measurements of closed-system natural zircon samples. Chemical Geology, 275, 186–198. https://doi.org/10.1016/j.chemgeo.2010.05.007

Maurer, F., Van Buchem, F. S. P., Eberli, G. P., Pierson, B. J., Raven, M. J., Larsen, H., Al-Husseini, M. I., & Vincent, B. (2013). Late Aptian long-lived glacio-eustatic lowstand recorded on the Arabian Plate. Terra Nova, 25, 87–94. https://doi.org/10.1111/ter.12009.

McHone, J. (1992). Mafic dike suites within Mesozoic igneous provinces of New England and Atlantic Canada. In J. H. Puffer & P. C. Ragland (Eds.), Eastern North American Mesozoic Magmatism (pp. 1–11): Geological Society of America Special Paper 268.

Meijer Drees, N. C. (1994). Devonian Elk Point Group of the Western Canada Sedimentary Basin. In G. Mossop and I. Shetsen (Eds.), Atlas of the Western Canada Sedimentary Basin (pp. 129–148): Canadian Society of Petroleum Geology and Albtera Research Council. https://ags.aer.ca/reports/atlas-western-canada-sedimentary-basin

Mitchell, C. E., Adhya, S., Bergström, S., Joy, M. P., & Delano, J. W. (2004). Discovery of the Ordovician Millbrig K-bentonite bed in the Trenton Group of New York State: implications for regional correlation and sequence stratigraphy in eastern North America. Paleogeography, Paleoclimatology, Paleoecology, 210, 331–346. https://doi.org/10.1016/j.palaeo.2004.02.037

Miles, B. D., Kukulski, R. B., Raines, M. K., Zonneveld, J. P., Leier, A. L., & Hubbard, S. M. (2012). A stratigraphic framework for Late Jurassic-Early Cretaceous gas-bearing strata (Monteith Formation) in the subsurface of northwest Alberta. Bulletin of Canadian Petroleum Geology, 60, 3–36. https://doi.org/10.2113/gscpgbull.60.1.3

Monger, J. W. H., & Gibson, H. D. (2019). Mesozoic-Cenozoic deformation in the Canadian Cordillera: the record of a "Continental Bulldozer"?. Tectonophysics, 757, 153–169. https://doi.org/10.1016/j.tecto.2018.12.023

Monger, J. W. H., & Price, R. A. (2002). The Canadian Cordillera: Geology and Tectonic Evolution. Canadian Society of Exploration Geophysicists Recorder February 2002, 17–36.

Monger, J. W. H., Souther, J. G., & Gabrielse, H. (1972). Evolution of the Canadian Cordillera: a plate-tectonic model. American Journal of Science, 272, 577–602. https://doi.org/10.2475/ajs.272.7.577

Moore, P. F. (1988). Devonian reefs in Canada and some adjacent areas. In H. H. J. Geldsetzer, N. P. James, and G. E. Tebbutt (Eds.), Reefs, Canada and Adjacent Area (pp. 367–390): Canadian Society of Petroleum Geologists.

Mossop, G. D., & Flach, P. D. (1983). Deep channel sedimentation in the Lower Cretaceous McMurray Formation, Athabasca oil sands, Alberta. Sedimentology, 30, 493–509. https://doi.org/10.1111/j.1365-3091.1983.tb00688.x

Mossop, G. D., & Shetsen, I. (1994a). Atlas of the Western Canada Sedimentary Basin. Canadian Society of Petroleum Geology and Albtera Research Council. https://ags.aer.ca/reports/atlas-western-canada-sedimentary-basin

Mossop, G. D., & Shetsen, I. (1994b). Introduction to the geological atlas. In G. Mossop, and I. Shetsen (Eds.), Atlas of the Western Canada Sedimentary Basin (pp. 1–11): Canadian Society of Petroleum Geology and Albtera Research Council. https://ags.aer.ca/reports/atlas-western-canada-sedimentary-basin

Moynihan, D. P., & Pattison, D. R. M. (2013). Barrovian metamorphism in the central Kootenay Arc, British Columbia: Petrology and isograd geometry. Canadian Journal of Earth Sciences, 50, 769–794. https://doi.org/10.1139/cjes-2012-0083

Netzeband, G. L., Gohl, K., Hübscher, C. P., Ben-Avraham, Z., Dehghani, G. A., Gajewski, D., & Liersch, P. (2006). The Levantine Basin-crustal structure and origin. Tectonophysics, 418, 167–188. https://doi.org/10.1016/j.tecto.2006.01.001

Odin, G. S., Barbin, V., Hurford, A. J., Baadsgaard, H., Galbrun, B., & Gillot, P. Y. (1991). Multi-method radiometric dating of volcano-sedimentary layers from northern Italy: age and duration of the Priabonian stage. Earth and Planetary Science Letters, 106, 151–168. https://doi.org/10.1016/0012-821X(91)90069-T

Oliver, J. (1986) Fluids expelled tectonically from orogenic belts: Their role in hydrocarbon migration and other geologic phenomena. Geology, 14, 99–102. https://doi.org/10.1130/0091-7613(1986)14<99:FETFOB>2.0.CO;2

Pană, D. I. (2021). 40Ar/39Ar dating of phyllonite in the Southern Rocky Mountain Trench and adjacent Rocky Mountains unravel kinematic links between the Omineca and Foreland Belts of the Southern Canadian Cordillera. The Journal of Geology, 129, 255–281. https://doi.org/10.1086/715243

Pană, D. I., Poulton, T. P., & DuFrane, S. A. (2019). U-Pb detrital zircon dating supports Early Jurassic initiation of the Cordilleran foreland basin in southwestern Canada. Geological Society of America Bulletin, 131, 318–334. https://doi.org/10.1130/B31862.1

Pană, D. I., & van der Pluijm, B. A. (2015). Orogenic pulses in the Alberta Rocky Mountains: radiometric dating of major faults and comparison with the regional tectono-stratigraphic record. Bulletin of the Geological Society of America, 127, 480–502. https://doi.org/10.1130/B31069.1

Pemberton, S. G., Flach, P. D., & Mossop, G. D. (1982). Trace fossils from the Athabasca oil sands, Alberta, Canada. Science, 217, 825–827. https://doi.org/10.1126/science.217.4562.825

Peng, Y., Hagstrom, C. A., Horner, S. C., Hodgson, C. A., Harrison, K. M., Leckie, D. A., Pedersen, P. K., & Hubbard, S. M. (2022). Low-accommodation foreland basin response to long-term transgression: a record of change from continental-fluvial and marginal-marine to open-marine sequences over 60,000 km^2 in the western Canada foreland basin. Marine and Petroleum Geology, 139, 1–20. https://doi.org/10.1161/j.marpetgeo.2022.105583

Pe-Piper, G., & Jansa, L.F. (1987). Geochemistry of late Middle Jurassic–Early Cretaceous igneous rocks on the eastern North American margin. GSA Bulletin, 99, 803–813. https://doi.org/10.1130/0016-7606(1987)99<803:GOLMJC>2.0.CO;2

Pe-Piper, G., Jansa, L. F., & Palacz, Z. (1994). Geochemistry and regional significance of the early Cretaceous bimodal basalt-felsic associations on Grand Banks, eastern Canada. Geological Society of America Bulletin, 106, 1319–1331. https://doi.org/10.1130/0016-7606(1994)106<1319:GARSOT>2.3.CO;2

Pe-Piper, G., & Piper, D. J. W. (2010). Volcanic ash in the Lower Cretaceous Chaswood Formation of Nova Scotia: Source and implications. Canadian Journal of Earth Sciences, 47, 1427–1443. https://doi.org/10.1139/E10-078

Porter, J. W., Price, R. A., & McCrossan, R. G. (1982). The Western Canada Sedimentary Basin. Philosophical Transactions of the Royal Society of London A, 305, 169–192. https://doi.org/10.1098/rsta.1982.0032

Price, R. A. (1994). Cordilleran tectonics and the evolution of the Western Canadian Sedimentary Basin. In G. Mossop, and I. Shetsen (Eds.), Atlas of the Western Canada Sedimentary Basin (pp. 13–24): Canadian Society of Petroleum Geology and Albtera Research Council. https://ags.aer.ca/reports/atlas-western-canada-sedimentary-basin

Quinn, G. M., Hubbard, S. M., Putnam, E., Matthews, W. A., Daniels, B. G., & Guest, B. (2018). A Late Jurassic to Early Cretaceous record of orogenic wedge evolution in the Western Interior basin, USA and Canada. Geosphere, 14, 1187–1206. https://doi.org/10.1130/GES01606.1

Quinn, G. M., Hubbard, S. M., van Drecht, R., Guest, B., Matthews, W. A., & Hadlari, T. (2016). Record of orogenic cyclicity in the Alberta foreland basin, Canadian Cordillera. Lithosphere, 8, 317–332. https://doi.org/10.1130/l531.1

Raines, M. K., Hubbard, S. M., Kukulski, R. B., Leier, A. L., & Gehrels, G. E. (2013). Sediment dispersal in an evolving foreland: detrital zircon geochronology from Upper Jurassic and lowermost Cretaceous strata, Alberta basin, Canada. Bulletin of the Geological Society of America, 125, 741–755. https://doi.org/10.1130/B30671.1

Ranger, M. (1994). A basin study of the southern Athabasca oil sands deposits [Ph.D. thesis]. University of Alberta, Edmonton. https://doi.org/10.7939/R3C53F644

Ranger, M. (2006). The Northeastern Sector of the Lower Cretaceous Athabasca Oil-Sands Basin: Facies and Fluids. In C. F. Gilboy and S. G. Whittaker (Eds.), Saskatchewan and Northern Plains Oil & Gas Symposium 2006 (Special Publications 19, pp. 238–248): Saskatchewan Geological Society.

Ranger, M.J., & Pemberton, S.G (1992). Sedimentology and ichnology of estuarine point bars in the McMurray Formation of the Athabasca oil sands deposit, northeastern Alberta, Canada. In S.G. Pemberton (Ed.), Applications of Ichnology to Petroleum Exploration: A core Workshop (pp. 401–421): Society for Sedimentary Geology. https://doi.org/10.3390/en12091769

Ranger, M. J., & Pemberton, S. G. (1997). Elements of a stratigraphic framework for the McMurray Formation in South Athabasca area, Alberta. In S. G. Pemberton, and D. P. Janes (Eds.), Petroleum Geology of the Cretaceous Mannville Group, Western, Canada (pp. 263–291): Canadian Society of Petroleum Geologists.

Reid, L. (2002). Stratigraphy, structure, petrology, geochronology and geochemistry of the Hobson Lake area (Cariboo Mountains, British Columbia) in relation to the tectoni evolution of the southern Canadian Cordillera [Ph.D. thesis] University of Calgary, Calgary. http://dx.doi.org/10.11575/PRISM/13461

Rinke-Hardekopf, L., Dashtgard, S. E., & MacEachern, J. A. (2019). Earliest Cretaceous transgression of North America recorded in thick coals: McMurray sub-basin, Canada. International Journal of Coal Geology, 204, 18–33. https://doi.org/10.1016/j.coal.2019.01.011

Rinke-Hardekopf, L., Dashtgard, S. E., Huang, C. & Gibson, H. D. (2021). Application of grouped detrital zircon analyses to determine provenance and closely approximate true depositional age: Early Cretaceous McMurray-Clearwater succession, Canada. Geoscience Frontiers, 12, 877–892. https://doi.org/10.1016/j.gsf.2020.11.016

Rinke-Hardekopf, L., Dashtgard, S. E., MacEachern, J. A., & Gingras, M. K. (2022). Resolving stratigraphic architecture and constraining ages of paralic strata in a low-accommodation setting, Firebag Tributary, McMurray Formation, Canada. The Depositional Record, 8, 754–785. https://doi.org/10.1002/dep2.181

Root, K. G. (2001). Devonian Antler fold and thrust belt and foreland basin development in the southern Canadian Cordillera: implications for the Western Canada Sedimentary Basin. Bulletin of Canadian Petroleum Geology, 49, 7–36. https://doi.org/10.2113/49.1.7

Ross, G. M., Patchett, P. J., Hamilton, M., Heaman, L., DeCelles, P. G., Rosenberg, E., & Giovanni, M. K. (2005). Evolution of the Cordilleran orogen (southwestern Alberta, Canada) inferred from detrital mineral geochronology, geochemistry, and Nd isotopes in the foreland basin. Geological Society of America Bulletin, 117, 747–763. https://doi.org/10.1130/B25564.1

Rossignol, C., Hallot, E., Bourquin, S., Poujol, M., Jolivet, M., Pellenard, P., Ducassou, C., Nalpas, T., Heilbronn, G., Yu, J. Dabard, M.-P. (2019). Using volcaniclastic rocks to constrain sedimentation ages: To what extent are volcanism and sedimentation synchronous?. Sedimentary Geology, 381, 46–64. https://doi.org/10.1016/j.sedgeo.2018.12.010

Schaltegger, U., Schmitt, A. K., & Horstwood, M. S. A. (2015). U-Th-Pb zircon geochronology by ID-TIMS, SIMS, and laser ablation ICP-MS: recipes, interpretations, and opportunities. Chemical Geology, 402, 89–110. https://doi.org/10.1016/j.chemgeo.2015.02.028

Schoene, B. (2014). U-Th-Pb Geochronology, In H. D. Holland, H. D. and K. K. Turekian (Eds.), Treatise on Geochemistry (pp. 341–378): Elsevier Ltd. https://doi.org/10.1016/B978-0-08-095975-7.00310-7

Schwartz, J. J., Johnson, K., Mueller, P., Valley, J., Strickland, A., & Wooden, J. L. (2014). Time scales and processes of Cordilleran batholith construction and high-Sr/Y magmatic pulses: Evidence from the Bald Mountain batholith, northeastern Oregon. Geosphere, 10, 1456–1481. https://doi.org/10.1130/GES01033.1

Sharman, G. R., & Malkowski, M. A. (2020). Needles in a haystack: Detrital zircon U-Pb ages and the maximum depositional age of modern global sediment. Earth-Science Reviews, 203, 103109. https://doi.org/10.1016/j.earscirev.2020.103109

Siégel, C., Bryan, S. E., Allen, C. M., & Gust, D. A. (2018). Use and abuse of zircon-based thermometers: A critical review and a recommended approach to identify antecrystic zircons. Earth-Science Reviews, 176, 87–116. https://doi.org/10.1016/j.earscirev.2017.08.011

Sigloch, K. & M. G. Mihalynuk (2013). Intra-oceanic subduction shaped the assembly of Cordilleran North America. Nature, 496, 50–56. https://doi.org/10.1038/nature12019

Sigloch, K. & M. G. Mihalynuk (2017). Mantle and geological evidence for a Late Jurassic–Cretaceous suture spanning North America. GSA Bulletin, 129, 1489–1520. https://doi.org/10.1130/B31529.1

Stockmal, G. S. (1984). Modeling of large-scale accretionary wedge and thin-skinned thrust-and-fold belt mechanics [Ph.D. thesis]. Brown University, Rhoad Island. https://doi.org/10.1029/JB088iB10p08271

Tepper, J. H., Nelson, B. K., Bergantz, G. W., & Irving, A. J. (1993). Petrology of the Chilliwack batholith, North Cascades, Washington: generation of calc-alkaline granitoids by melting of mafic lower crust with variable water fugacity. Contributions to Mineralogy and Petrology, 113, 333–351. https://doi.org/10.1007/BF00286926

Theriault, F. (1988). Lithofacies, diagenesis and related reservoir properties of the Upper Devonian Grosmont Formation, northern Alberta. Bulletin of Canadian Petroleum Geology, 36, 52–69. https://doi.org/10.35767/gscpgbull.36.1.052

Underschultz, J. R., & Erdmer, P. (1991). Tectonic loading in the Canadian Cordillera as recorded by mass accumulation in the foreland basin. Tectonics, 10, 367–380. https://doi.org/10.1029/90TC02442

Vakarelov, B. K., & Bhattacharya, J. P. (2009). Local tectonic control on parasequence architecture: Second Frontier sandstone, Powder River Basin, Wyoming. American Association of Petroleum Geologists Bulletin, 93, 295–327. https://doi.org/10.1306/10150807015

Van Wagoner, J. C., Mitchum, R. M., Campion, K. M., & Rahmanian, V. D. (1990). Siliciclastic sequence stratigraphy in well logs, core, and outcrops: concepts for high resolution correlation of time and facies. American Association of Petroleum Geologists Methods in Exploration Series, 7, 1–55. https://doi.org/10.1306/mth7510

Vermeesch, P. (2004). How many grains are needed for a provenance study?. Earth and Planetary Science Letters, 224, 441–451. https://doi.org/10.1016/j.epsl.2004.05.037.

Vermeesch, P. (2021). Maximum depositional age estimation revisited. Geoscience Frontiers, 12, 843–850. https://doi.org/10.1016/j.gsf.2020.08.008.

Wahbi, A. M., Blum, M. D., & Doerger, C.N., (2022). Early Cretaceous continental-scale sediment routing, the McMurray Formation, Western Canada Sedimentary Basin, Alberta, Canada. Geological Society of America Bulletin, 135, 1–19. https://doi.org/10.1130/b36412.1

Wang, X., Griffin, W. L., & Chen, J. (2010)., Hf contents and Zr/Hf ratios in granitic zircons. Geochemical Journal, 44, 65–72. https://doi.org/10.2343/geochemj.1.0043

Webster, E. R., & Pattinson, D. R. M. (2014). U-Pb Dates for the Nelson and Bayonne Magmatic Suites in the Salmo-Creston Area, Southeastern British Columbia: Tectonic Implications for the Southern Kootenay Arc (Parts of NTS 082F/02,/03,/06,/07). In Geoscience BC Summary of Activities 2013. Geoscience BC, Report 2014-1, 99–114.

Weleschuk, Z. P., & Dashtgard, S. E. (2019). Evolution of an ancient (Lower Cretaceous) marginal-marine system from tide-dominated to wave-dominated deposition, McMurray Formation. Sedimentology, 66, 2354–2391. https://doi.org/10.1111/sed.12601

Wheeler, H. E., & Mallory, V. S. (1953). Designation of stratigraphic units. American Association of Petroleum Geologists Bulletin, 37, 2407–2421. https://doi.org/10.1306/5ceadd9d-16bb-11d7-8645000102c1865d

Wightman, D. M., & Pemberton, S. G. (1997). The Lower Cretaceous (Aptian) McMurray Formation: an overview of the Fort McMurray area, northeastern Alberta. In S. G. Pemberton & D. P. James (Eds.), Petroleum Geology of the Cretaceous Mannville Group, Western, Canada (pp. 312–344): Canadian Society of Petroleum Geologists.

Yoshida, S. (2000). Sequence and facies architecture of the upper Blackhawk formation and the lower castlegate sandstone (Upper Cretaceous), Book Cliffs, Utah, USA. Sedimentary Geology, 136, 239–276. https://doi.org/10.1016/S0037-0738(00)00104-4.

Zaitlin, B. A., Warren, M. J., Ptoocki, D., Rosenthal, L., & Boyd, R. (2002). Depositional styles in a low accommodation foreland basin setting: an example from the Basal Quartz (Lower Cretaceous), southern Alberta. Bulletin of Canadian Peroleum Geology, 50, 31–72. https://doi.org/10.2113/50.1.31

How to cite: Fietz, S. W., Crowley, J. L., MacEachern, J. A., Dashtgard, S. E., & Gibson, H. D. (2023). Geochronology of reworked ash and its implications for accommodation space variations in distal foreland basins, McMurray Formation, Alberta, Canada. Sedimentologika, 1(1), 1-17. https://doi.org/10.57035/journals/sdk.2023.e11.1131